

# **Mechanically Controlled Liesegang Pattern Formation in Stretchable Polyacrylamide Gels for Elastic Deformation Tracking**

A THESIS SUBMITTED TO  
THE GRADUATE SCHOOL OF ENGINEERING AND  
SCIENCE  
OF BILKENT UNIVERSITY  
IN PARTIAL FULFILLMENT OF THE REQUIREMENTS  
FOR  
THE DEGREE OF  
MASTER OF SCIENCE  
IN CHEMISTRY

By

Mohammad Morsali

July 2019

# Mechanically Controlled Liesegang Pattern Formation in Stretchable Polyacrylamide Gels for Elastic Deformation Tracking

By Mohammad Morsali

July 2019

We certify that we have read thesis and that in our opinion it is fully adequate, in scope and in quality, as a thesis for the degree of Master of Science.

---

Bilge BAYTEKIN (Advisor)

---

Ferdi KARADAŞ

---

Istvan LAGZI

---

Salih ÖZÇUBUKÇU

---

Emrah ÖZENSOY

Approved for the Graduate School of Engineering and Science:

---

Ezhan KARAŞAN  
Director of the Graduate School

## ABSTRACT

### Mechanically Controlled Liesegang Pattern Formation in Stretchable Polyacrylamide Gels for Elastic Deformation Tracking

Mohammad Morsali

M.S. in Chemistry

Advisor: Bilge BAYTEKIN

July 2019

Pattern formation in nature has been intellectually appealing for many scientists since antiquity. Simultaneous diffusion and reaction of chemicals in gel media may lead to precipitation and complex pattern formation through self-assembly. Periodic precipitations patterns, also known as Liesegang patterns (LP), are one of the stimulating examples of such self-assembling reaction-diffusion systems. So far, it was shown that LP's periodic band structure and their unique geometry can be controlled by controlling the reaction parameters (e.g. concentration of the reactants) and affecting the reaction medium (e.g. external electrical field). However, so far, the research on LPs have been concentrated mostly around how these patterns are forming, to retrieve information to build a universal mathematical model for them. Although there are studies showing the effect of external fields on the development of these patterns, to the best of our knowledge, so far, there is no example of these systems, used to retrieve information about the changes in the environment as they form.

Here, we first show the formation of Liesegang rings by a diffusion-precipitation reaction in a stretchable hydrogel. Then, we present how to use these patterns to 'read' the duration, the extent, and the direction of gel deformation. Also, we describe deviations from LP behavior for the patterns (spacing that can be mathematically defined by a geometrical series) formed after the unloading. We believe this first display of such an 'environmental sensing' to be a starting point for more investigations on many aesthetically appealing and mathematically challenging self-assembled systems, which have been studied for decades.

**Keywords:** Liesegang pattern, post-pattern, hydrogel, elastic deformation.

## ÖZET

Esneyebilen Poliakrilamid Jellerde Elastik Deformasyonun Takip Edilmesi İçin Mekanik Kontrollü Liesegang Halkaları Oluşumu

Mohammad Morsali

Kimya, Yüksek Lisans

Tez danışmanı: Bilge Baytekin

Temmuz 2019

Doğadaki desen oluşumu, antik çağlardan beri birçok bilim insanının ilgisini çekmiştir. Kimyasalların eş zamanlı difüzyon ve jel ortamında reaksiyona girmesi ve kendiliğinden bir araya gelmesi çökelmeye ve karmaşık desen oluşumunu sağlayabilir. Liesegang halkaları (LH) olarak da bilinen periyodik çökeltme desenleri, bu tür kendiliğinden oluşan reaksiyon difüzyon sistemlerinin dikkat çekici örneklerinden biridir. Şimdiye kadar, LH'nin periyodik bant yapısının ve kendine özgü geometrilerinin, reaksiyon parametrelerini kontrol ederek (örneğin, tepkiyen konsantrasyonu) ve tepkime ortamının (örneğin, harici elektrik alanı) özelliklerini değiştirerek kontrol edilebildiği gösterilmiştir. Bununla birlikte, şu ana kadar LH'ler üzerindeki araştırmalar -halkalar için evrensel bir matematik model oluşturmak için bilgi edinmek amacıyla- çoğunlukla bu desenlerin nasıl oluştuğu üzerine yoğunlaşmıştır. Her ne kadar dış etki alanların bu halkaların büyümesine etkisini gösteren çalışmalar olsa da, şu ana kadar literatürde bu sistemlerde halkaların oluştuğu çevrede meydana gelen değişiklikler hakkında bilgi almak için LH'leri kullanan hiçbir örnek yoktur.

Bu çalışmada, ilk defa esneyebilen bir hidrojelde difüzyon-çökeltme reaksiyonu ile Liesegang halkalarının oluşumunu göstermekteyiz. Ardından, bu desenlerin jel deformasyonunun süresini, kapsamını ve yönünü gözlemlemek için nasıl kullanılacağını açıklamaktayız. Ayrıca, mekanik gerilmenin ortadan kaldırılmasından sonra oluşan desenlerin (geometrik bir seri ile matematiksel olarak tanımlanabilen aralık) LH davranışından sapmalarını ortaya koymaktayız. Böyle bir “çevresel algılama”nın ilk kez ortaya konmasının, onlarca yıldır incelenen, estetik açıdan çekici

ve matematiksel olarak açıklanması zor olan bu sistemler hakkında daha fazla araştırma için bir başlangıç noktası olduğuna inanmaktayız.

**Anahtar Kelimeler** : Liesegang halkaları, sonradan oluşan halkalar, hidrojel, elastik deformasyon

## **ACKNOWLEDGMENT**

First of all, I would like to express my sincere gratitude to my supervisor Assoc. Prof. Bilge Baytekin for all of her support, guidance, patience and great supervision during this research. I also want to thank Assoc. Prof. Tarik Baytekin for his feedback and support.

I am grateful to Assoc. Prof. Istvan Lagzi for his valuable support and guidance during this research and being a great host during my research visit at Budapest University of Technology and Economics.

Special thanks to all of my colleagues and friends, Rahym Ashirov, Doruk Cezan and Turab Ali Khan for their help and assisting me in experiments. I would like to thank Mertcan Ozel for his help, friendship and support during my stay at Bilkent University. Many thanks to Dr. Joanna Kwiczak Yigitbasi, Dr. Fatma Demir, Mine Demir for being supportive colleagues and great friends.

I acknowledge TÜBİTAK for providing financial support under project no: 116Z116.

*To Bilge Baytekin*  
*The real wonder woman*

## TABLE OF CONTENTS

1. INTRODUCTION .....	1
1.1. Chemistry and mathematics of LPs.....	4
1.2. The internal and external factors effecting the formation of LPs .....	7
1.3. Hydrogel media mechanically and chemically appropriate for the formation of LP patterns and the simultaneous application of the mechanical input upon LP formation .....	8
1.4. Preliminary work on the LP formation in stretchable hydrogels .....	9
1.5. The ‘post-pattern’ phenomenon .....	13
2. MATERIALS AND METHODS .....	14
2.1. Materials.....	14
2.2. Preparation of polyacrylamide (PAA) hydrogels with primarily-added $K_2CrO_4$ content .....	15
2.3. Preparation of polyacrylamide (PAA) hydrogels with secondarily-added potassium chromate content.....	16
2.4. Preparation of 3D polyacrylamide-sodium alginate hybrid hydrogel.....	17
2.5. Preparation of the 3D agarose gels.....	17
2.6. Preparation of the agarose stamp .....	18
2.7. Preparation of the Ecoflex substrate .....	18
2.8. The experimental setup for mechanical deformation in 1D and 2D gels.....	19
2.9. Chemical erasing of the LPs formed in the hydrogels .....	20
2.10. Polymerization of pyrrole on LP patterns .....	20
2.11. Optical imaging .....	20



2.12. Image processing and analysis .....	20
3. RESULTS AND DISCUSSION .....	22
3.1. Formation of post-patterns in 1D, 2D, and 3D PAA hydrogels.....	22
3.1.1 Formation of post-patterns in 2D PAA hydrogels .....	22
3.1.2 Formation of post-patterns in 1D PAA hydrogels .....	28
3.1.3 Formation of LP and post-patterns in 3D hydrogels.....	34
3.1.3.1 Formation of post-patterns in 3D agarose gels .....	34
3.1.3.2 Formation of LP and post-patterns in 3D polyacrylamide-alginate hybrid gels.....	36
3.2. Elastic Deformation Tracking in 1D, 2D, and 3D hydrogels by using precipitation patterns.....	40
3.2.1 Determination of the tensile strain in an elastically deformed 2D hydrogel using post-patterns .....	40
3.2.2 Precipitation patterns in an elastically deformed 2D hydrogel under cyclic load.....	41
3.2.3 Precipitation patterns in an elastically deformed 1D hydrogel under cyclic load.....	45
3.3. Removing patterns .....	48
3.4. Pyrrole polymerization on the previously formed precipitation patterns.....	48
4. CONCLUSION.....	51
5. REFERENCES.....	53

## **LIST OF TABLES**

Table 1. The transition times used to yield different cycles of elastic deformation to obtain the precipitation patterns shown in Figure 20.  $T_{\text{end}}=12$  hours (fixed).....43

## LIST OF FIGURES

Figure 1. Examples of Liesegang patterns. (a) Periodic pattern formation in a volcanic rock [9], reprinted with permission from [10]. (b) The formation of **2D** LPs in the polyacrylamide hydrogel presented in this work. (c) Generic mathematical equations governing LPs. *The pattern in (b); Inner electrolyte (chromate ion) = 0.01 M, outer electrolyte (copper (II) ion) = 1 M, acrylamide = 13.5 w%, BIS = 0.056 w%, KPS = 0.187 w%, TEMED = 0.0001 w%. T = 20 °C. For details, please see chapter 2. ....* 1

Figure 2. Scheme of a reaction-diffusion system formed by wet stamping in a hydrogel resulting in formation of LPs [11]. (a) Diffusion of outer electrolyte, **A**, (with a higher concentration than the inner electrolyte) in the hydrogel media doped with inner electrolyte, **B**. (b) Tentative concentration profiles of outer (**B**) and inner electrolytes (**A**) and precipitations formed in LP system (**A** diffuses from ‘left to right’). (c) Close-up photos of the time lapse of LP formation in the polyacrylamide hydrogel. *Inner electrolyte (chromate ion) = 0.01 M, outer electrolyte (copper (II) ion) = 1 M, acrylamide = 13.5 w%, BIS = 0.056 w%, KPS = 0.187 w%, TEMED = 0.0001 w%. T = 20 °C. For details, please see chapter 2.....* 3

Figure 3. Simulation of Liesegang patterns in **1D** using partial differential equations (PDEs) described in ((1-1)~(1-4)) as dimensionless models using a self-developed code in MATLAB by spatial discretization technique using ode45 ODE solver . (a) Formation of sharp periodic precipitations using the qualitative dimensionless model. (b) Peak analysis of the simulated precipitation by identifying the peak positions. (c) Spacing law validation in the model. According to the ‘spacing law’ for LPs, the consecutive peaks positions ( $X_n$ ) and peaks number (n) should follow the equation  $Ln(X_n)/n = Ln(1 + p)$  – as shown in (c) this model successfully predicts/reproduces such a case..... 6

Figure 4. Chemical structure of polyacrylamide hydrogel. (a) Acrylamide monomer (AA) chemical structure. (b) N,N-Methylenebis(acrylamide) cross-linker (BIS) a.k.a. ‘bis-acrylamide’. (c) Covalently cross-linked polyacrylamide hydrogel (PAA). Adopted from ref. [51]. .....9

Figure 5. Concentric LP formation in stretched polyacrylamide hydrogel and the change in its geometry (from circle to oval) after unloading and releasing the stress. *Inner electrolyte (chromate ion) = 0.01 M, outer electrolyte (copper (II) ion) = 1 M, acrylamide = 13.5 w%, BIS = 0.056 w%, KPS = 0.187 w%, TEMED = 0.0001 w%. T = 20 °C.* ..... 10

Figure 6. Formation of Liesegang patterns (LPs) upon loading for 24 hrs and just after unloading at the 24th hr. The photos of LPs in gels with 0-50% strain, (a) upon loading for 24 hrs, and (b) just after unloading the stress at the 24th hr. Loading for 24 hours does not affect (c) the minor axis length of the final rings, (d) the estimated number of the rings formed, and (e) spacing coefficient ( $1+p$ ) in different sets of samples. However, upon unloading LP appearances change significantly as displayed by the (f) changes in the aspect ratio (a) and (b). *Inner electrolyte (potassium chromate) = 0.01 M, outer electrolyte (copper chloride) = 1 M, acrylamide = 13.5 w%, BIS = 0.056 w%, KPS = 0.187 w%, TEMED = 0.0001 w%. T = 20 °C.* ..... 12

Figure 7. Formation of post-patterns in polyacrylamide (PAA) hydrogel with 40% strain upon loading for 24 hrs and unloading for 18 hrs. (photo taken 18 hours after the unloading). *Inner electrolyte (potassium chromate) = 0.01 M, outer electrolyte (copper chloride) = 1 M, acrylamide = 13.5 w%, BIS = 0.056 w%, KPS = 0.187 w%, TEMED = 0.0001 w%. T = 20 °C.* ..... 13

Figure 8. The plexiglass molds dimensions and shapes. (a) Plexiglass mold interior and its dimensions used for casting ‘**2D**’ rectangular hydrogels. (b) Comb-like plexiglass mold interior and its dimensions for casting three ‘**1D**’ hydrogels at the same time. (c) The hydrogel casted and formed in ‘**1D**’ mold with  $K_2CrO_4$  as inner electrolyte. *Plexiglass thickness = 2 mm.* ..... 15

Figure 9. Preparation and cast molding of polyacrylamide (PAA) hydrogel. (a) Acrylamide (AA) and Bis-acrylamide (BIS) are dissolved in deionized water. (b) Solution is degassed under vacuum for 20 minutes. (c) KPS and  $K_2CrO_4$  are added and mixed carefully to the solution not to introduce further oxygen in the sample. (d) Addition of TEMED and gelation initiation in prepared solution after addition of

TEMED. (e and f) Casting of solution in plexiglass mold before first gelation stage complete using syringe. ....	16
Figure 10. Preparation of the <b>3D</b> polyacrylamide-sodium alginate hybrid hydrogel. (a) Dissolving 0.15 g sodium alginate (SA) in 30 ml deionized water in ice bath. (b) Mixing sodium alginate solution and polyacrylamide (PAA) hydrogel precursors (8.676 g acrylamide (AA), 0.036 g Bis-acrylamide (BIS), 0.12 g of potassium peroxydisulfate (KPS) and 0.12 g $K_2CrO_4$ ) dissolved in 25.2 ml deionized water. (c) Addition of 120 $\mu$ L TEMED as catalyst to start gelation. (d) Pouring solution to polystyrene (PS No. 6) cuboid molds (4 cm $\times$ 4 cm $\times$ 4 cm).....	17
Figure 11. Schematic illustration of <b>2D</b> uniaxial stretching setup. (a) Transferring hydrogel on Ecoflex substrate. (b) Loading (stretching) sample, followed by stamp placing at the center of the hydrogel. (c) Formation of the patterns on the hydrogel upon loading. (d) The sample unloading.....	19
Figure 12. Gray-value analysis of Liesegang patterns in Figure 13a. (a) Gray-value profile of LPs in loading (stretching) direction just before unloading. (b) Peaks analysis of gray-value profile including peaks intensities, widths (full width at half maximum) and peak <i>prominences</i> (difference between gray-value of bands and their neighbor depletion zone).....	21
Figure 13. A typical demonstration of PP formation in <b>2D</b> hydrogel. (a-c) The patterns of $CuCrO_4$ formed by diffusion of $Cu^{2+}$ into $CrO_4^{2-}$ containing polyacrylamide (PAA) gel during and after elastic deformation of the gel. (a) Formation of patterns in a stretched (40% strain) PAA hydrogel after 24 hours. (b) The change in the aspect ratio of patterns after unloading (releasing) the stress. (c) Post-patterns formed in the sample after unloading (release) (photo taken 18 hours after unloading). <i>Inner electrolyte (potassium chromate) = 0.01 M, outer electrolyte (copper chloride) = 1 M, acrylamide = 13.5 w%, BIS = 0.056 w%, KPS = 0.187 w%, TEMED = 0.0001 w%. T = 20 °C. For details of the gel preparation and loading setup please see Chapter 2. ....</i>	23
Figure 14. Gray-value profile of the patterns of $CuCrO_4$ formed by diffusion of $Cu^{2+}$ (1 M) into $CrO_4^{2-}$ (0.01 M) containing polyacrylamide gel during and after elastic deformation of the gel (close-up of the patterns in loading (stretching) direction in Figure 13c). During the 24-hour loading, regular LP1 form. Post-pattern (PP) and LP2 regions form after unloading (releasing) the sample (18 <sup>th</sup> hour after unloading). <i>Inner electrolyte (potassium chromate) = 0.01 M, outer electrolyte (copper chloride) = 1 M, acrylamide = 13.5 w%, BIS = 0.056 w%, KPS = 0.187 w%, TEMED = 0.0001 w%. T</i>	

= 20 °C. 40 % strain upon loading for 24 hrs. Photo taken in 18 hours after unloading. For details of the gel preparation and loading setup please see Chapter 2. ....24

Figure 15. Differences between the patterns formed after unloading (PP) and the regular LP formed during loading (LP1) and long after unloading (LP2). (a) Gray-value analyses of the patterns of CuCrO<sub>4</sub> formed by diffusion of Cu<sup>2+</sup> (1 M) into CrO<sub>4</sub><sup>-</sup> (0.01 M) containing polyacrylamide gel during and after elastic deformation of the gel (data retrieved from the gray-value analysis of the image shown in Figure 14). Changes in (b) the width of patterns, (c) the spacing of the two consecutive bands, (d) the peak prominence (difference between gray-value of bands and their neighbor depletion zone). ....26

Figure 16. Gray-value profile of precipitation patterns upon loading at the 4th hour and unloading at the 6th hour. Stamp is placed on an unloaded polyacrylamide (PAA) hydrogel. After 4 hours of LP formation, the sample is loaded (stretched) up to 40 % strain. PPs and LP2s are led to develop, then sample is unloaded after 2 hours and the photo is taken after 6 hours. *Inner electrolyte (potassium chromate) = 0.01 M, outer electrolyte (copper chloride) = 1 M, acrylamide = 13.5 w%, BIS = 0.056 w%, KPS = 0.187 w%, TEMED = 0.0001 w%. T = 20 °C. For details of the gel preparation and the loading setup please see Chapter 2. ....27*

Figure 17. Gray-value analyses of the PP and LP2 displayed in Figure 16. (a) Gray-value profile. Changes in (b) the width of patterns, (c) the spacing of the two consecutive bands, (d) the peak prominence (difference between gray-value of bands and their neighbor depletion zone). (here, LP1 are not shown since their line spacings are too small to be detected by gray-value analyses)). ....28

Figure 18. Schematic illustration of the steps involved in the preparation of the setup for **1D** Liesegang pattern formation. (a) Placing polyacrylamide (PAA) hydrogel on Ecoflex substrate. (b) Loading and stretching PAA hydrogel. (c) Placing cuboid stamp at the center of the PAA hydrogel. (d) **1D** Liesegang patterns forms as parallel bands. Note that the length of the stamp should be the same as the hydrogel width to obtain these parallel precipitation patterns. ....29

Figure 19. The formation of precipitation patterns in **1D** gels, the effect of uniaxial, tensile elastic deformation on the pattern formation in the polyacrylamide (PAA) gel. (a) Formation of LPs in Agarose (Agarose, 8 w%). (b) LPs formed in a reference (unloaded) PAA hydrogel (*acrylamide = 13.5 w%, BIS = 0.056 w%, KPS = 0.187 w%, TEMED = 0.0001 w%. T = 20 °C*) after 12 hours. (c) LPs formed in the loaded (40%

strain) PAA sample after 12 hours. (d) ‘Shrinking’ of LPs in the reverse direction of the previous tension in the PAA just after unloading. (e) Formation of PPs and LP2s in PAA hydrogel after unloading, in 12 hours. (f-g) Gray-value profiles of LPs developed in the reference and the loaded PAA gel after 12 hours of loading. *In both Agarose and PAA hydrogels: Inner electrolyte (potassium chromate) = 0.01 M, outer electrolyte (copper chloride) = 1 M. For details of the gel preparation and the loading setup please see Chapter 2.*.....30

Figure 20. Demonstration of the stretching and the compressing functions. Elastic mechanical deformation can be explained mathematically using so called stretching and compressing functions. If  $f(x)$  represent (red) concentration profile in a medium,  $f(0.5x)$  represents (yellow) the concentration profile in the case of ‘shrinkage’ with -50% strain (can be analogue to stretched/released transformation) and  $f(2x)$  shows (blue) concentration profile upon stretching the sample with 50% strain (unstretched/stretched transition)......32

Figure 21. The formation of PP in **1D** polyacrylamide (PAA) gels loaded to 10-50% strain. LP formed during 12 hours of loading; after unloading, 12 hours of waiting generates PP and LP2. *Inner electrolyte (potassium chromate) = 0.01 M, outer electrolyte (copper chloride) = 1 M, acrylamide = 13.5 w%, BIS = 0.056 w%, KPS = 0.187 w%, TEMED = 0.0001 w%. T = 20 °C. For details of the gel preparation and loading setup please see Chapter 2.*.....33

Figure 22. Time evolution of the precipitation patterns in a **1D** PAA gel with LP1s already developed (Figure 21d). LP formed for 12 hours and the consecutive photos are showing time evolution of pattern formation (PPs and LPs) after unloading the stress. The patterns were developed for further 8 hours, images were taken every 30 minutes. *For details of the gel preparation and loading setup please see Chapter 2.* .....33

Figure 23. Formation of precipitation patterns in **3D** in 8 w% agarose sphere. (a) Agarose sphere removed from 1 M  $K_2CrO_4$  outer electrolyte solution. (b) Cross section of **3D** sample. (c) Thin layer cut from sample for rings detection. *Inner electrolyte (copper chloride) = 0.01 M, outer electrolyte (potassium chromate) = 1 M, T=20 °C. For details of the gel preparation please see Chapter 2.* .....34

Figure 24. The formation of **3D** patterns in an agarose hydrogel hemisphere (diameter = 4 cm) using wet stamping method. (a) Patterns formed after 24 hours. (b) Top view of sample without stamp. (c) Cross section of sample after cutting to halves. (d) Thin

film cut of cross section for rings detection. <i>Inner electrolyte (potassium chromate) = 0.01 M, outer electrolyte (copper chloride) = 1 M. T = 20 °C. For details of the gel preparation please see Chapter 2.</i> .....	35
Figure 25. Cracks formed in presence of 20% mechanical deformation (compression) in cubic agarose sample (a). Thin layers of sample for rings detection (b). <i>Agarose = 8 w%, Inner electrolyte (potassium chromate) = 0.01 M, outer electrolyte (copper chloride) = 1 M, T = 20 °C. For details of the gel preparation and loading setup please see Chapter 2.</i> .....	36
Figure 26. Effect of mold surface modification on final <b>3D</b> polyacrylamide-sodium alginate (PAA-SA) hybrid hydrogel. (a) PAA-SA, gel molded without filter paper. (b) PAA-SA hydrogels molded with filter paper. In (b) demolding is easy for both samples but in the sample with dry filter paper, separation of the gel and the filter paper is not possible. Finally, the best configuration is using CaCl <sub>2</sub> , for which both demolding and removal of the paper are straightforward. <i>Inner electrolyte (potassium chromate) = 0.01 M, acrylamide = 13.5 w%, BIS = 0.056 w%, KPS = 0.187 w%, sodium alginate = 0.187 w%, TEMED = 0.0001 w%. T = 20 °C. For details of the gel preparation please see Chapter 2.</i> .....	37
Figure 27. Formation of LP in the <b>3D</b> polyacrylamide-sodium alginate (PAA-SA) hybrid hydrogel. The cylindrical stamp is place on the surface of the cube-shaped gel. Developing time was 24 hrs. The chemistry and the concentration of inner and outer-electrolyte are similar to <b>1D</b> and <b>2D</b> PAA hydrogels. <i>Inner electrolyte (potassium chromate) = 0.01 M, acrylamide = 13.5 w%, BIS = 0.056 w%, KPS = 0.187 w%, sodium alginate = 0.187 w%, TEMED = 0.0001 w%. T = 20 °C. For details of the gel preparation please see Chapter 2.</i> .....	38
Figure 28. Mechanical deformation setup in <b>3D</b> . (a) <b>3D</b> polyacrylamide-sodium alginate (PAA-SA) hydrogel. (b) Isometric view of compression test setup. (c) Top view of compressed gel with stamp placed. <i>Compression = 30 %. Inner electrolyte (potassium chromate) = 0.01 M, outer electrolyte (copper chloride) = 1 M, acrylamide = 13.5 w%, BIS = 0.056 w%, KPS = 0.187 w%, sodium alginate = 0.187 w%, TEMED = 0.0001 w%. T = 20 °C. For details of the gel preparation and the loading setup please see Chapter 2.</i> .....	38
Figure 29. formation of patterns in <b>3D</b> polyacrylamide-sodium alginate (PAA-SA) gel after 24 hours with 30% compression. Concentric shell patterns form, (a) top, (b) side	



and (c) bottom view of the hemispherical patterns. *For details of the gel preparation and loading setup please see Chapter 2.*.....39

Figure 30. Photos of the LP formed upon loading and just after unloading (releasing) the compressive load. (a) Top view of pattern formed in polyacrylamide-sodium alginate (PAA-SA) **3D** hydrogel in 24 hours under a compressive load. (b) Aspect ratio of the pattern increases (from 1.0 to 1.30) in **3D** LP pattern right after unloading. *For details of the gel preparation and loading setup please see Chapter 2.* .....39

Figure 31. Formation of post-patterns in **3D** in the presence of mechanical deformation (30% compression). (a) LP patterns just after releasing the load. (b) Formation of post rings perpendicular to the stress direction, bottom view. (c) Side view of patterns perpendicular to the stress direction. (d) Side view of patterns in the stress direction. *Inner electrolyte (potassium chromate) = 0.01 M, outer electrolyte (copper chloride) = 1 M, acrylamide = 13.5 w%, BIS = 0.056 w%, KPS = 0.187 w%, sodium alginate = 0.187 w%, TEMED = 0.0001 w%. T = 20 °C. For details of the gel preparation and loading setup please see Chapter 2.*.....40

Figure 32. Post-pattern (PP) formation in the polyacrylamide (PAA) samples with applied uniaxial strain. (a) The change in the aspect ratios of the concentric LP1 formed for 24 hrs, photo taken just after unloading. (b) The formation of the PPs and LP2s (in 18 hours of waiting time) after unloading. (c) The effect of strain on the PP region's size and on the precipitation bands' width and contrast. *Inner electrolyte (potassium chromate) = 0.01 M, outer electrolyte (copper chloride) = 1 M, acrylamide = 13.5 w%, BIS = 0.056 w%, KPS = 0.187 w%, TEMED = 0.0001 w%. T = 20 °C. For details of the gel preparation and loading setup please see Chapter 2.* .....41

Figure 33. Pattern formation under cyclic loading. An example of a 3 step-cyclic elastic deformation of the PAA gel and the formation of the precipitation patterns. Formation of patterns in a) 4 hrs of unloaded gel, followed by b) a stretching, which causes an overall pattern shown in (c) after 4 hrs of loading. The sample is then unloaded as shown in (d) and the patterns were left to develop for 4 hrs more in the unloaded state to yield the pattern in (e). (Here the photos are given in gray scale for a better contrast.) *Inner electrolyte (potassium chromate) = 0.01 M, outer electrolyte (copper chloride) = 1 M, acrylamide = 13.5 w%, BIS = 0.056 w%, KPS = 0.187 w%, TEMED = 0.0001 w%. T = 20 °C. For details of the gel preparation and loading setup please see Chapter 2.* .....42

Figure 34. Cyclic deformation in **2D** polyacrylamide (PAA) hydrogels. Samples are mechanically loaded/unloaded (stretched/released) in x-direction through cycles as shown in (a); Vertical axis 0 = unloaded (released/unstretched), and 1 = loaded (stretched) sample. (b) Overall patterns formed during the corresponding loading cycles. (c) A magnification of the patterns formed in cyclic loading and unloading (x-direction). (d) Peak analysis of the PP formed, including peak width and prominence analysis of PP (e) PP formation in y-direction (perpendicular to uniaxial loading) (The photos are given in gray-scale for better contrast). *Inner electrolyte (potassium chromate) = 0.01 M, outer electrolyte (copper chloride) = 1 M, acrylamide = 13.5 w%, BIS = 0.056 w%, KPS = 0.187 w%, TEMED = 0.0001 w%. T = 20 °C. For details of the gel preparation and the loading setup please see Chapter 2. ....44*

Figure 35. Cyclic deformation in **1D** polyacrylamide (PAA) hydrogels. Samples are mechanically loaded/unloaded (stretched/released) in x-direction through cycles as shown in (a); Vertical axis 0 = unloaded (released/unstretched), and 1 = loaded (stretched) sample. (b) The patterns formed in cyclic loading and unloading (x-direction). *Inner electrolyte (potassium chromate) = 0.01 M, outer electrolyte (copper chloride) = 1 M, acrylamide = 13.5 w%, BIS = 0.056 w%, KPS = 0.187 w%, TEMED = 0.0001 w%. T = 20 °C. For details of the gel preparation and loading setup please see Chapter 2. ....46*

Figure 36. A detailed demonstration of the PP formation in cyclic loading and unloading. (a) Magnified view of the patterns shown in Figure 35. (b) Peak prominence and (c) peak width analysis of the patterns. *Inner electrolyte (potassium chromate) = 0.01 M, outer electrolyte (copper chloride) = 1 M, acrylamide = 13.5 w%, BIS = 0.056 w%, KPS = 0.187 w%, TEMED = 0.0001 w%. T = 20 °C. For details of the gel preparation and loading setup please see Chapter 2. ....47*

Figure 37. Polymerization of pyrrole on polyacrylamide (PAA) hydrogel with LPs formed. (a-b) Polypyrrole formation on regular LPs. (c-d) Polypyrrole formation on the patterns developed on mechanically deformed hydrogel. Peak analysis of LP formed on PAA (e) without mechanical deformation, and (f) with mechanical deformation. In all cases, the samples with patterns were dipped in pyrrole solution (pyrrole = 0.1 M, HCl = 0.1 mM). *Inner electrolyte (potassium chromate) = 0.01 M, outer electrolyte (copper chloride) = 1 M, acrylamide = 13.5 w%, BIS = 0.056 w%, KPS = 0.187 w%, TEMED = 0.0001 w%. T = 20 °C. For details of the gel preparation please see Chapter 2. ....49*



## **LIST OF ABBREVIATIONS**

<b>LP</b>	Liesegang pattern
<b>PP</b>	Post-pattern
<b>PAA</b>	Polyacrylamide
<b>SA</b>	Sodium alginate
<b>AA</b>	Acrylamide
<b>BIS</b>	N,N'-methylene(bis)acrylamide
<b>KPS</b>	Potassium peroxydisulfate
<b>TEMED</b>	N,N,N',N'-tetramethylethylenediamine
<b>LU</b>	Loading/unloading
<b>UL</b>	Unloading/loading
<b>1D, 2D and 3D</b>	One, two and three dimensional

## CHAPTER 1

### 1. INTRODUCTION

Self-assembly has been a topic of interest among researchers as it provides autonomous organization of components in a system without external manipulation of individual components in detail [1]. There are few self-assembling and pattern evolving systems as a result of the processes, which would be expected to bring more homogeneity rather than a periodic heterogeneous state [2]. Liesegang patterns (**LPs**) are one of the examples of spontaneous pattern formation [3], formed by reaction-diffusion (diffusion coupled to the reaction of chemicals), which leads to the periodic bands of precipitation [4] (Figure 1). These periodic structures follow specific mathematical laws [5] including time law [6], spacing law [7], and width law [8] which make them unique and distinguishable from other periodic pattern forming phenomena.

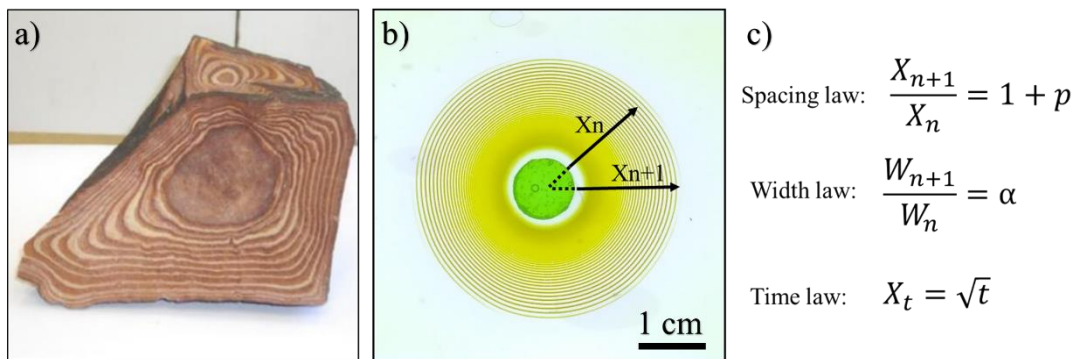


Figure 1. Examples of Liesegang patterns. (a) Periodic pattern formation in a volcanic rock [9], reprinted with permission from [10]. (b) The formation of **2D** LPs in the polyacrylamide hydrogel presented in this work. (c) Generic mathematical equations governing LPs. *The pattern in (b); Inner electrolyte (chromate ion) = 0.01 M, outer*

*electrolyte (copper (II) ion) = 1 M, acrylamide = 13.5 w%, BIS = 0.056 w%, KPS = 0.187 w%, TEMED = 0.0001 w%. T = 20 °C. For details, please see chapter 2.*

Hydrogels have been chosen as reaction medium to monitor the formation of reaction-diffusion patterns in many literature examples, since they provide a necessary medium for the diffusion of the system components, minimize the convection, and provide a stable environment for the retention of the formed pattern. To form a Liesegang pattern, in addition to a hydrogel medium, two inter diffusing components (called as electrolytes) which can react to form a precipitate are necessary. In Figure 2, we describe a system, in which the formation of the LP is done in a virtually **2D (planar)** fashion (Figure 2). In this system, the length of the third dimension of the gel (the height) is much smaller than the other two, so the patterns can be visualized from the ‘top’, as if they are forming in a plane. Conventionally, wet stamping method is used to bring the two reactants together in such a ‘**2D**’ system for a systematic and clear monitoring of the event and the effect of some experimental parameters on it, i.e. the concentration of the reactants. The reactant, which is supplied from outside (through another gel called as ‘stamp’) into gel medium is known as the *outer electrolyte* and the reactant, which is doped homogeneously in the gel medium is known as the *inner electrolyte* [11], Figure 2. For a reaction-diffusion system to produce LPs, there should be large difference (10 to 100 times) between the concentration of inner and outer electrolytes. Putting the stamp soaked with the outer electrolyte (**A**) on the hydrogel previously doped with inner electrolyte (**B**) (Figure 2a), will lead to the diffusion of **A** into the hydrogel media. In the classic theory of this phenomenon [12] as **A** diffuses into the gel, its concentration rises in the medium. Simultaneously, **A** reacts with **B**, forming the water-insoluble reaction product, **P**. The amount of the product increases as the reaction proceeds and reaches a threshold necessary for the precipitation. At this point, **P** precipitates. The interplay between the diffusion (continuously carrying more **A** into the hydrogel) and the reaction between **B** and **A**, forming product **P** that depletes **A** and **B** concentrations, leads to changes in the concentration gradients of **A** and **B** in hydrogel media. As a result, such a reaction-diffusion system leads to a periodic structure, in which the ‘circles’ or ‘bands’ are the places, where **P** forms in the highest amounts (Figure 2b).

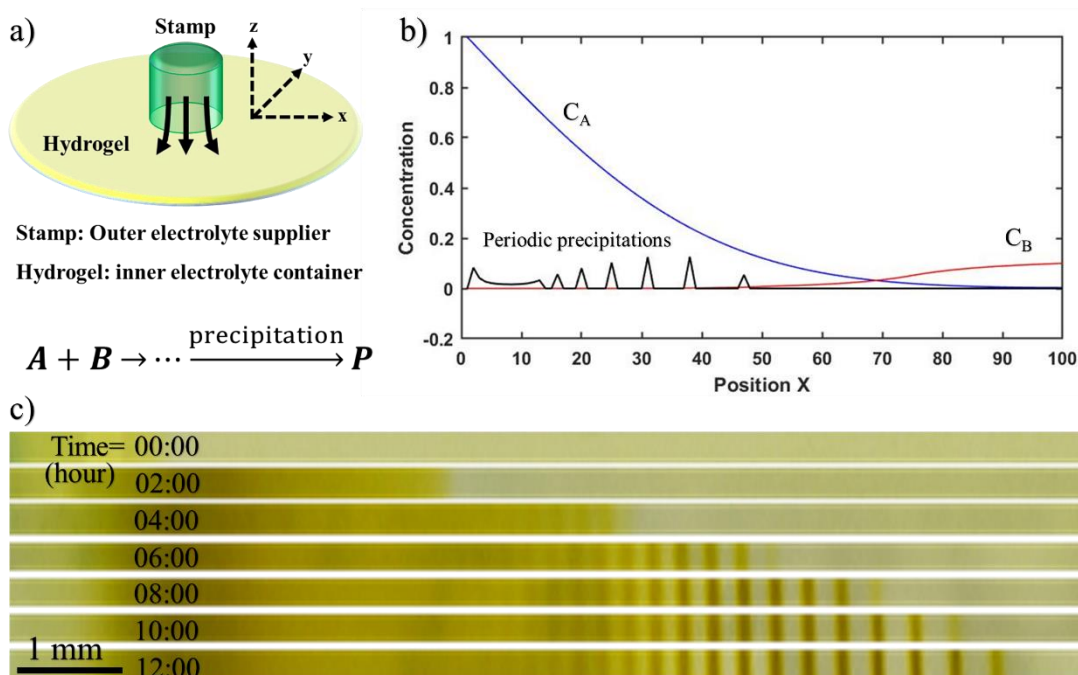


Figure 2. Scheme of a reaction-diffusion system formed by wet stamping in a hydrogel resulting in formation of LPs [11]. (a) Diffusion of outer electrolyte, **A**, (with a higher concentration than the inner electrolyte) in the hydrogel media doped with inner electrolyte, **B**. (b) Tentative concentration profiles of outer (**B**) and inner electrolytes (**A**) and precipitations formed in LP system (**A** diffuses from ‘left to right’). (c) Close-up photos of the time lapse of LP formation in the polyacrylamide hydrogel. *Inner electrolyte (chromate ion) = 0.01 M, outer electrolyte (copper (II) ion) = 1 M, acrylamide = 13.5 w%, BIS = 0.056 w%, KPS = 0.187 w%, TEMED = 0.0001 w%.  $T = 20$  °C. For details, please see chapter 2.*

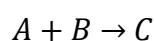
LPs can be encountered frequently in nature [13–15]. Their aesthetical beauty and complex nature attracted the attention of many scientists. Since their discovery [16], they have been proposed for many applications [15] like sensors, colloidal and surface sciences, bioengineering and microfluidics, and fabrication of microstructure materials alongside other pattern formation techniques [17]. However, so far no ‘real’ application of such LPs has been truly realized. LPs can be observed in different geometries of the hydrogels than the ‘**2D**’ [11] described above. Formation of LPs in different hydrogels and with other electrolytes in ‘**1D**’ (in vertical test tubes) by simple solution diffusion [18,19], and in **3D** are described in the literature [20]. LPs were also reported to form in systems in water vapor [21], and also in the absence of water [22],

which endowed the belief that many reaction-diffusion systems can be engineered to form periodic precipitation [23].

### 1.1. Chemistry and mathematics of LPs

Chemical systems that form unusual visual patterns has always been at the center of attention of scientists and mathematicians. For example, Alan Turing, one the greatest mathematicians of all times, tried to formulate many pattern-forming system in nature [24] and the temporal evolution of patterns. LPs, with their characteristic spacing, width, and time laws, are different than Turing patterns and are formed by other chemical mechanisms [25]. Generally, models describing formation of LPs can be classified into two; *pre-nucleation* and *post-nucleation* [26]. In the pre-nucleation model, pattern formation is the result of a perturbation of the diffusion by nucleation. Nucleation takes place, when the system becomes supersaturated and reaches a critical point, at which the system in a far-from equilibrium state transforms to its equilibrium state [27]. In the post-nucleation model, the precipitation region is the result of competitive growth of precipitate and ends in a phase separation and an uneven distribution of the precipitate [4,26,28]. In post-nucleation model, it is not necessary for nucleation and precipitation to occur at the same time and location. Nucleation will result in the formation of homogenously distributed sol of colloidal particles. Ostwald ripening occurs and larger particles grow while smaller particles get eliminated [12,29,30]. Although the two models proposed are mechanistically different, their mathematical descriptions are essentially similar [31]. In both models, the *diffusion* term can be expressed using Fick's second law and the *reaction* can be described either in the form of a mass action law, or a phase separation driven by Cahn-Hilliard or Gibbs-Thomson effect [26].

A simple chemical mechanism [32] is based on the pre-nucleation and supersaturation theory, which describes the production of precipitates through a two-step mechanism incorporating an intermediate species. This mechanism can be written as:



where **A** and **B** are outer and inner electrolytes, and **C** is the intermediate product, which can transform to precipitate **P**. Usually, the initial condition is such that the



concentration of the outer electrolyte (**A**) is much higher than that of the inner electrolyte (**B**); thus, the pattern formation is governed by the diffusion front of the outer electrolyte. In this model, **C** forms continuously behind the chemical front as a result of mass action law (1-3), and **C** can transform to immobile precipitate, **P**, if the local concentration of **C** reaches a nucleation threshold. The precipitate can grow further by further deposition of **P** at this point. This precipitation process is much faster than the diffusion of the chemical species; therefore, the distinct LP bands can form. These processes can be written in the form of a set of partial differential equations, which describe the evolution of the patterns.

$$\frac{\partial a}{\partial t} = D_a \nabla_x^2 a - \frac{\partial c}{\partial t} - \frac{\partial p}{\partial t} \quad (1-1)$$

$$\frac{\partial b}{\partial t} = D_b \nabla_x^2 b - \frac{\partial c}{\partial t} - \frac{\partial p}{\partial t} \quad (1-2)$$

$$\frac{\partial c}{\partial t} = \theta(a \cdot b - ab^*)(1 - \theta(p)) \times k \cdot a \cdot b \quad (1-3)$$

$$\frac{\partial p}{\partial t} = \theta(c - c^*) \times k \cdot a \cdot b \quad (1-4)$$

where **a**, **b**, **c** and **p** are concentration of inner electrolyte (**A**), outer electrolyte (**B**), intermediate product (**C**) and final precipitation formed (**P**), respectively. **D<sub>a</sub>** and **D<sub>b</sub>** show diffusion coefficient of **A** and **B**, and **θ** is the Heaviside function. **ab<sup>\*</sup>** is the thermodynamic threshold for formation of precipitate. **c<sup>\*</sup>** is the nucleation threshold, which is in the form of **a.b**; however with higher value and include the kinetics in precipitation phenomenon [33]. Using these equations in a self-developed MATLAB<sup>®</sup> code by spatial discretization and implementing ode45 ODE solver (designed for solving ordinary differential equations), we tried to qualitatively simulate the appearance of ‘**1D**’ LP lines. As shown in Figure 3, this mathematical model can reproduce the LP with corresponding line spacings and spacing coefficients. The periodic peaks plotted by the program obey the spacing law observed experimentally, that is the set of consecutive peak position obey  $X_{n+1}/X_n = 1 + p$  relation ( $Ln(X_n)/n = Ln(1 + p)$ ) when the pattern is completed. Note that, this model is not

capable of reproducing ‘the width law’, which can be observed experimentally, so the widths of the peaks displayed in Figure 3 are the size of space grid size ( $\Delta x$ ) and fixed in all peaks.

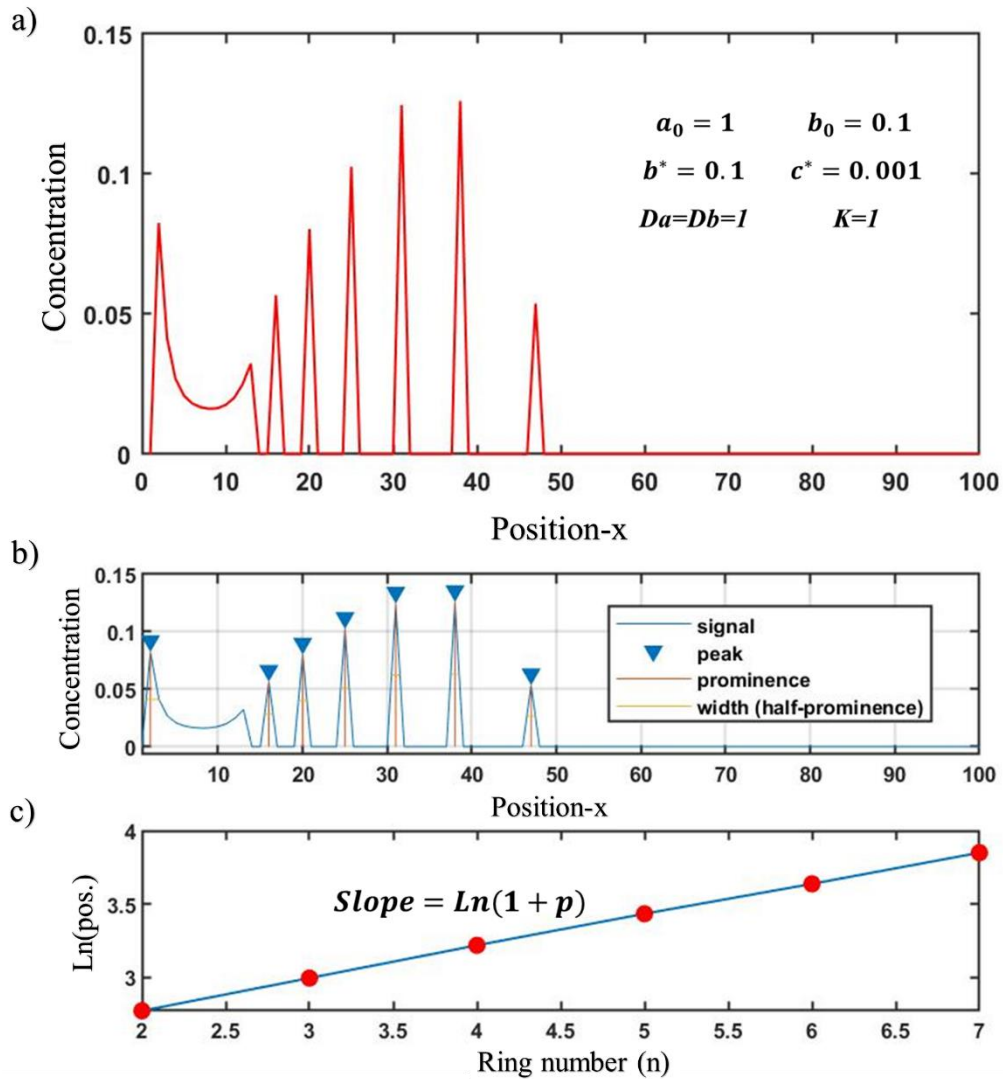


Figure 3. Simulation of Liesegang patterns in **1D** using partial differential equations (PDEs) described in ((1-1)~(1-4)) as dimensionless models using a self-developed code in MATLAB by spatial discretization technique using ode45 ODE solver . (a) Formation of sharp periodic precipitations using the qualitative dimensionless model. (b) Peak analysis of the simulated precipitation by identifying the peak positions. (c) Spacing law validation in the model. According to the ‘spacing law’ for LPs, the consecutive peaks positions ( $X_n$ ) and peaks number ( $n$ ) should follow the equation  $\text{Ln}(X_n)/n = \text{Ln}(1 + p)$  – as shown in (c) this model successfully predicts/reproduces such a case.

## 1.2. The internal and external factors effecting the formation of LPs

Matalon and Packter reported the effect of the concentration of the anions and the cations (the electrolytes), pH, the chemistry of the gel medium on the LP formation. They also reported a special case, in which an addition of chloride ion to a gelatin gel effects the LP formation in this gel [34]. Badr and Sultan described the effect of electrolyte concentrations on morphology of  $\text{Co(OH)}_2$  LPs [35]. The effect of the gel precursor concentration and the gel impurities, i.e., the presence of gelatin as impurity in agarose, on the spacing coefficient  $(1+p)$  of copper chromate LPs in agarose gel was also reported by Lagzi [32]. Shreif et al. reported a chemical modification for  $\text{Co(OH)}_2$  LPs, that clears the fuzzy precipitate region tracing at the back of the propagating pattern, which increases the LP ring spacings. In their study, they display the effect of three main parameters, which alters overall LP appearance: 1) Decreasing the concentration of the diffusing (outer) electrolyte ( $\text{NH}_4\text{OH}$ ), 2) Applying a constant radial electric field across the circular pattern, and 3) Increasing the gel concentration to a moderately high value. It is also possible to distort LPs morphology in a **2D** system by applying a linear electric field across the gel medium [36]. Toramaru et al. showed that concentration of the gel medium can highly affect the LPs morphology, e.g., in a Liesegang system forming lead iodide precipitate, in low concentrations of the agarose gel, tree-like morphologies can be observed instead of LPs. They also showed that tree-like morphologies can coexist with LPs in the medium concentrations of the gel precursor [37].

Kárpáti-Smidróczki et al. studied the effect of the degree of the crosslinker (glutaraldehyde) on the formation LPs in PVA gels [38]. Smoukov et al. showed the effect of UV-induced crosslinking of a dichromated gelatin via reduction of chromate ions. In this method, the amount of dichromate in inner electrolyte decreases and the gel become stiffer and as a result the heights of the surface undulations decreases [39]. There are other studies on the external control LP formation with electric fields [40–43] and microwave radiation [44].

Despite the extensive knowledge and numerous reports on internal and external effects on the LP formation as shown above, there is no study on the effect of mechanical deformation of the medium on LP formation. However, it is reasonable to think, an elastic deformation - that does not damage the gel's initial form upon loading and once the load is released - can be used to effect the formation of LPs. However,

for this, the conventional gel media for LP cannot be used, since none of these media, e.g., agarose, gelatin, are stretchable - they disintegrate even at small tensile or compressive loads. Therefore, new, stretchable gels are needed for such an operation. However, despite their emerging applications [45], most ‘stretchable gels’ also have weak mechanical properties and do not show high stretchability, e.g., alginate hydrogel can be stretched up to 20% strain until rupture and gelatin (at a swelling of 40 times) can be extended up to 11% strain to break [45,46]. Still, there are a few synthetic hydrogels including polyacrylamide (PAA), which show desirable mechanical properties with proper elasticity and can be stretched in the range of 10 to 20 times its original dimension (~1000 to 2000 % strain) [45]. Therefore, we used PAA in our experiments as the receiving gel medium, to probe the effect of mechanical deformation of the gel on the formation of the LP patterns.

### **1.3. Hydrogel media mechanically and chemically appropriate for the formation of LP patterns and the simultaneous application of the mechanical input upon LP formation**

The transparent polyacrylamide (PAA) gel enables the visual monitoring of the diffusion of charged species, which diffuse at moderate rates (measured in hours) in the gel, and therefore, has been used as a common electrophoresis medium [47–49]. PAA structure and the factors influencing its properties is well documented in the literature. The ratio of the total weight of monomers to the volume of the solution (%T) and the ratio of the mass of cross-linker to the total mass of monomers (%C) are reported to have significant impact on the swelling capacity and pore size of the gel, [49,50] which eventually affect the mechanical properties of the PAA hydrogel.

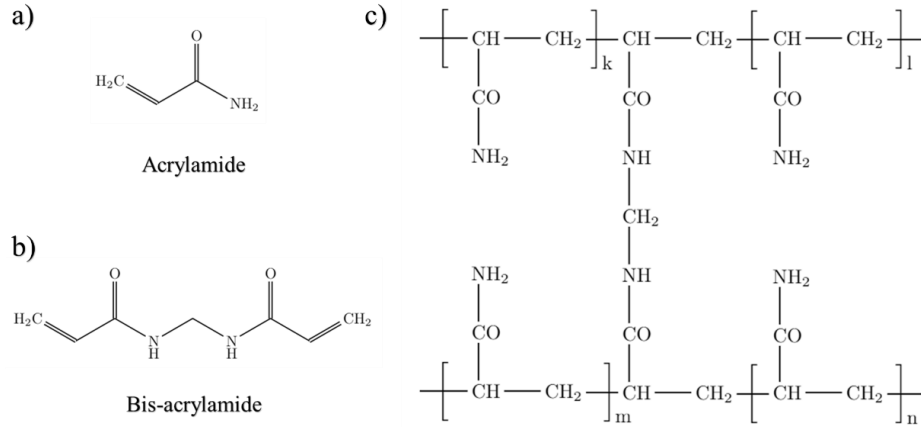


Figure 4. Chemical structure of polyacrylamide hydrogel. (a) Acrylamide monomer (AA) chemical structure. (b) N,N-Methylenebis(acrylamide) cross-linker (BIS) a.k.a. ‘bis-acrylamide’. (c) Covalently cross-linked polyacrylamide hydrogel (PAA). Adopted from ref. [51].

For a PAA gel to be suitable for a test of our hypothesis, it has to be both highly stretchable and strong. Therefore, the two experimental parameters, the water content (%T) and the cross-linker ratio (%C), had to be optimized, firstly. On the other hand, the addition of inner electrolyte (for forming LPs) to the hydrogel may also alter its stretchability and strength. For example, in our case, the doped PAA hydrogel with an inner electrolyte (chromate ions (0.01 M)), cross-linking and polymerization are hindered, which vitally effects the strength of the gel, due to the formation of hydrogen bonding [52] between chromate’s oxygen atoms and the hydrogens in the amide groups of the gel. In order to overcome this problem and regain gel integrity, addition of more cross-linker is then required.

$$\%T = \frac{m \text{ acrylamide } (g) + m \text{ crosslinker } (g)}{\text{total volume, ml}} \times 100 \quad (1-5)$$

$$\%C = \frac{m \text{ crosslinker } (g)}{m \text{ acrylamide } (g) + m \text{ crosslinker } (g)} \times 100 \quad (1-6)$$

#### 1.4. Preliminary work on the LP formation in stretchable hydrogels

In a preliminary work from our group [53], the above-mentioned gel parameters to obtain a stretchable and strong gel were optimized, in order to realize our target reaction-diffusion system, in which the gel medium will be subjected to a mechanical

input. Then, the most suitable reactions with a chemistry that is orthogonal to the groups present in the structure of the hydrogel reaction medium were determined. In one of the mechanically and chemically optimized systems, a **2D** setup of the PAA hydrogel (7 cm x 7 cm x 2 mm) was prepared, doped with  $K_2CrO_4$  (0.01 M, inner electrolyte) by addition of  $K_2CrO_4$  into PAA hydrogel precursors before gelation. The stamp, which contains 1.0 M of  $CuCl_2$  outer electrolyte, was prepared by soaking the stamp in the corresponding solution for 40 minutes. Then the doped gel was clamped on the stretching setup and the stamp was placed at the center of the PAA hydrogel, as shown in Figure 5. (see Experimental for further details of the hydrogel and the stamp preparation and the stretching setup). The gel was loaded a uniaxial tension to yield an elastic strain of 50%, and was let to stay in the loaded position (under stress) *as long as the LP patterns were developed* (24 hrs). (Strains up to 60% were found to cause only elastic deformation and no plastic deformation in this gel medium) An identically prepared but ‘not loaded’ sample was prepared in parallel, as a control sample. The LPs formed in the loaded (stretched) gel and the not-loaded (not stretched) control are almost identical in their positions relative to the stamp. This was shown to be the case for all the samples loaded to obtain strains of 10% to 50%. In other words, mechanical deformation has no effect on the LP formation on the stretched samples. The ratio of the final ring ‘diameters’ (the ratio of the highest (major) axis length to the lowest (minor) axis length, or ‘**the aspect ratios**’ - as we named it in this study - do not change for the stretched samples and is equal to 1 (meaning the LP has a circular shape), Figure 6a.

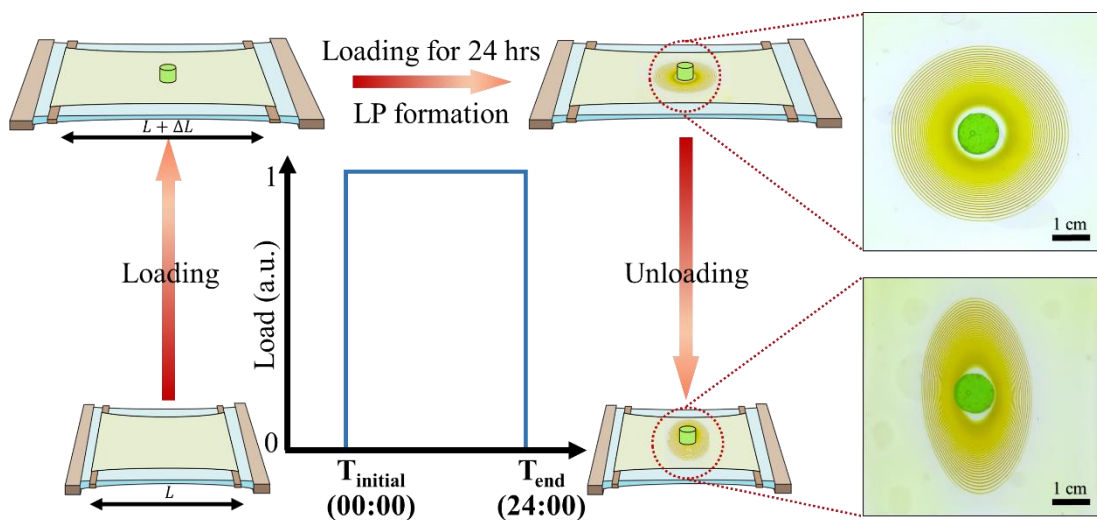


Figure 5. Concentric LP formation in stretched polyacrylamide hydrogel and the change in its geometry (from circle to oval) after unloading and releasing the stress.

*Inner electrolyte (chromate ion) = 0.01 M, outer electrolyte (copper (II) ion) = 1 M, acrylamide = 13.5 w%, BIS = 0.056 w%, KPS = 0.187 w%, TEMED = 0.0001 w%. T = 20 °C.*

The fact that same, circular concentric LP were observed and the LPs propagating front (diffusion front) was located at the same position (distance) with respect to the stamp, regardless of the different extent of strain applied on the hydrogel samples tells us that the diffusion phenomenon was not affected by the elastic mechanical input (Figure 6a). This was also verified by the observations that spacing and width laws were all valid for both the loaded and the control (not loaded) samples. Figure 6. (We should note here that ‘the number of the rings’, which has been one of the prominent parameters reported in the literature of LPs, produces high errors due to the difficulty in identifying the exact position and the number of the earlier rings (Figure 6d). Therefore, we used spacing coefficients  $(1+p)$ , which are  $X_{n+1}/X_n = 1 + p$ , and the aspect ratios of the final pattern for comparison of the LP patterns).

Upon releasing the load (unloading), however, the LPs formed on the stretched samples looked different than the control sample, which was not loaded (Figure 6). The visual difference between the loaded and not-loaded samples - which we expressed as the change in the aspect ratio - is proportional to the extent of strain; as illustrated in Figure 6f. Increasing the strain from 0% to 50%, the aspect ratio increased from 1 up to 1.74. Since the standard deviation of the aspect ratio vs. strain was found to be quite low, this type of information can also be used ‘reversely’; i.e. the aspect ratio of the LP in a sample can be used to estimate the elastic deformation that the sample went through upon formation of the LP. However, since the experimental parameters are quite specific for the given systems with LP formation, for such an operation on a new gel system, a ‘calibration curve’ has to be made to find the ‘unknown’ mechanical deformation.

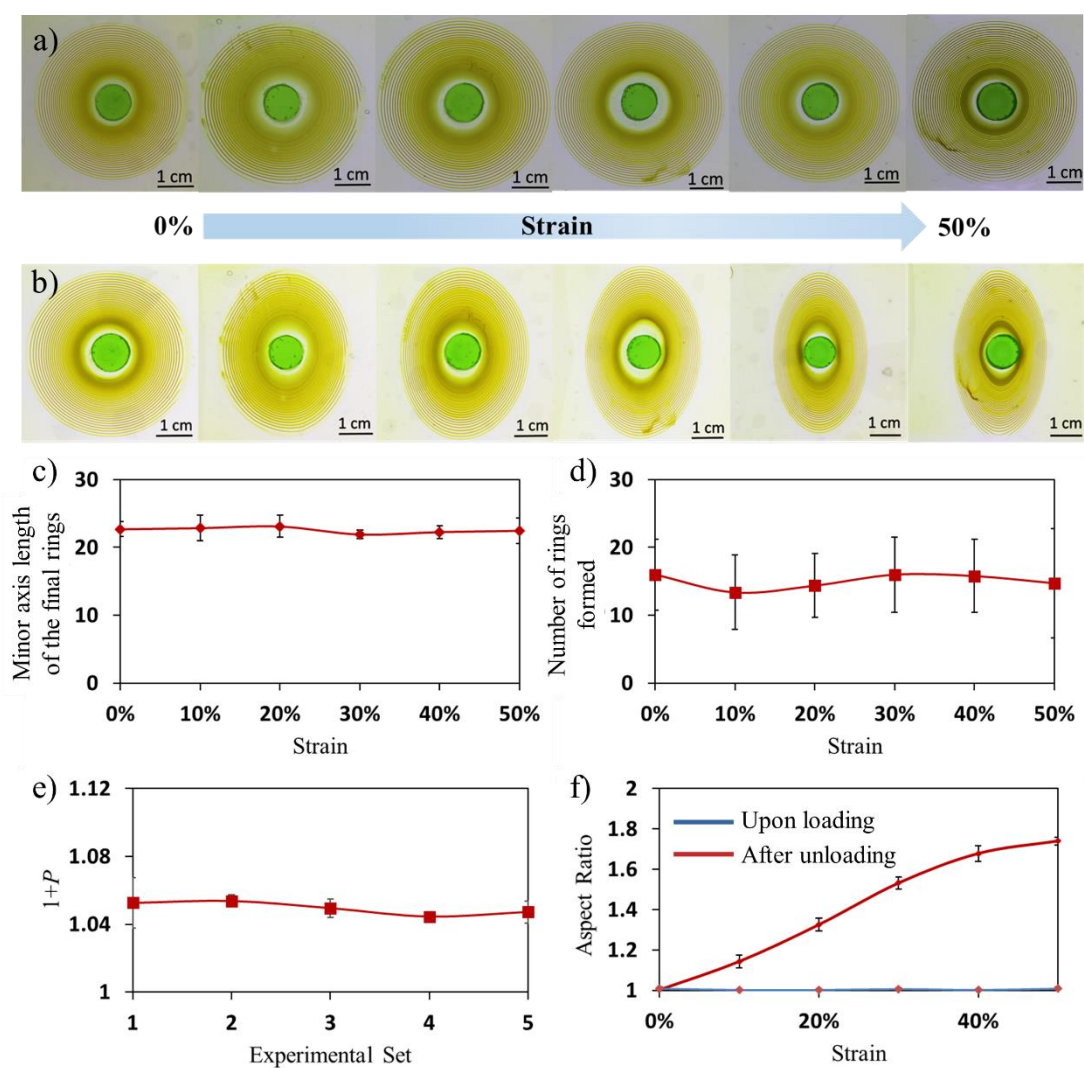


Figure 6. Formation of Liesegang patterns (LPs) upon loading for 24 hrs and just after unloading at the 24th hr. The photos of LPs in gels with 0-50% strain, (a) upon loading for 24 hrs, and (b) just after unloading the stress at the 24th hr. Loading for 24 hours does not affect (c) the minor axis length of the final rings, (d) the estimated number of the rings formed, and (e) spacing coefficient ( $1+p$ ) in different sets of samples. However, upon unloading LP appearances change significantly as displayed by the (f) changes in the aspect ratio (a) and (b). *Inner electrolyte (potassium chromate) = 0.01 M, outer electrolyte (copper chloride) = 1 M, acrylamide = 13.5 w%, BIS = 0.056 w%, KPS = 0.187 w%, TEMED = 0.0001 w%. T = 20 °C.*



## 1.5. The ‘post-pattern’ phenomenon

Despite all the models and simulations performed so far, there is still an urge for a complete description and a model which can describe the formation of periodic Liesegang patterns completely [26]. Reported irregularities like ‘secondary LPs’ - [30] can help to understand the reaction/diffusion phenomenon and to develop a more general model on LPs. While trying to observe and quantify the effect of mechanical deformation on the change of ovality of concentric LPs, we serendipitously noticed such an interesting irregularity in the pattern formation: When the reaction/diffusion system was let to continue to form patterns, by waiting 18 hours *additionally after the unloading*, new patterns with different and visually distinguishable structures than regular LPs developed (Figure 7). It was also noted that these new patterns were formed with stamp or after its removal upon unloading. As we show below, these irregular patterns proved to be very useful in tracking of mechanical deformation in the gel. Since the patterns were formed *after* the deformation has taken place, we named them as “**post-patterns (PP)**”.

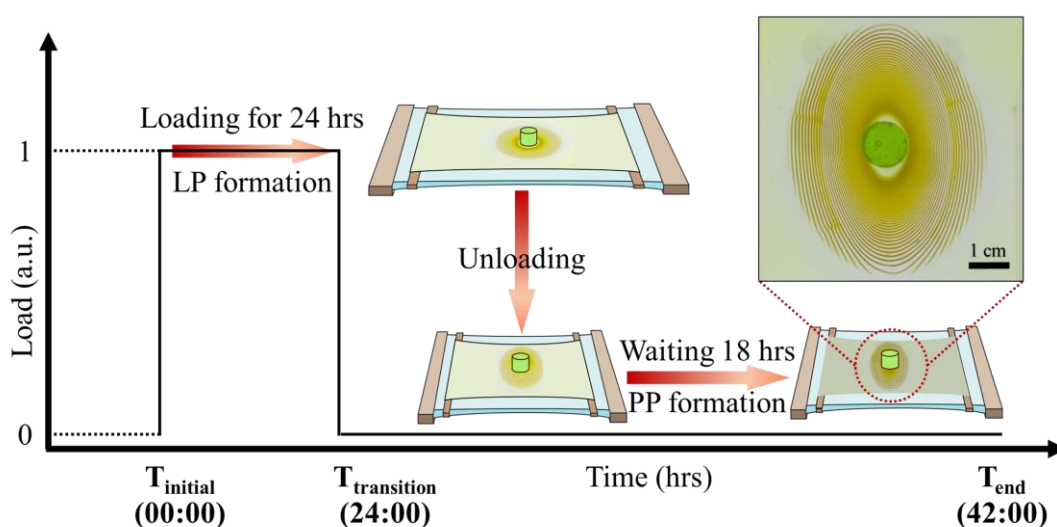


Figure 7. Formation of post-patterns in polyacrylamide (PAA) hydrogel with 40% strain upon loading for 24 hrs and unloading for 18 hrs. (photo taken 18 hours after the unloading). *Inner electrolyte (potassium chromate) = 0.01 M, outer electrolyte (copper chloride) = 1 M, acrylamide = 13.5 w%, BIS = 0.056 w%, KPS = 0.187 w%, TEMED = 0.0001 w%. T = 20 °C.*

## CHAPTER 2

### 2. MATERIALS AND METHODS

#### 2.1. Materials

Acrylamide (AA) (Sigma-Aldrich, 98 % purity), N,N'-methylene(bis)acrylamide (BIS) (Sigma-Aldrich, 99% purity), potassium peroxydisulfate (KPS) (Sigma-Aldrich, 99 % purity), sodium alginate (Acros organics), N,N,N',N'-tetramethylethylenediamine (TEMED) (Sigma-Aldrich, 99% purity), agarose (Fisher bioreagents, for analysis purposes), pyrrole (Sigma-Aldrich, density = 0.967 g/ml), potassium chromate (Merck, 99.5 %), copper (II) chloride dihydrate (Merck, 99 % purity), calcium chloride dihydrate (Merck, 99 % purity), acetic acid glacial (Carlo erba), hydrochloric acid (Carlo erba, 37 %) and ammonia solution (Vwr, 25 %) were used as supplied.

Plexiglass, Parafilm® and Ecoflex® 00-30 (Smooth-On, Inc.) were used without any chemical modification.

#### **Mold preparation for '1D' and '2D' hydrogels**

For casting of the hydrogels (PAA and agarose), the molds were prepared by cutting plexiglass using a laser cutter (Universal Laser System®, VLS3.50 Desktop). Two plexiglass sheets (9.5 cm × 9.0 cm × 2 mm), which served as the exteriors of the mold, were covered with Parafilm to facilitate the hydrogel removal after the formation of the gel. Another plexiglass sheet was cut into desired shape (rectangle for **2D** and comb-like for **1D**) with dimensions shown in Figure 8, and was sandwiched between the exterior sheets.

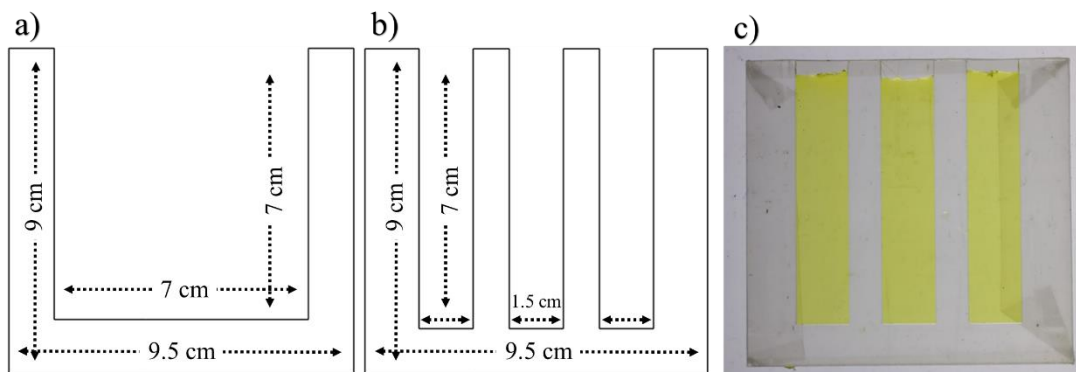


Figure 8. The plexiglass molds dimensions and shapes. (a) Plexiglass mold interior and its dimensions used for casting ‘**2D**’ rectangular hydrogels. (b) Comb-like plexiglass mold interior and its dimensions for casting three ‘**1D**’ hydrogels at the same time. (c) The hydrogel casted and formed in ‘**1D**’ mold with  $K_2CrO_4$  as inner electrolyte. *Plexiglass thickness = 2 mm.*

## 2.2. Preparation of polyacrylamide (PAA) hydrogels with primarily-added $K_2CrO_4$ content

1.446 g acrylamide (AA) and 0.006 g bis-acrylamide (BIS) were dissolved in 9.2 ml deionized water. The solution was degassed under vacuum for 20 minutes. 0.02 g of potassium peroxydisulfate and 0.02 g potassium chromate were added and mixed carefully not to introduce further oxygen in the sample. Immediately after addition and mixing of 20  $\mu$ L TEMED, prepared hydrogels were casted in the plexiglass molds. Samples were stored in room temperature for 24 hrs for complete gelation to occur.

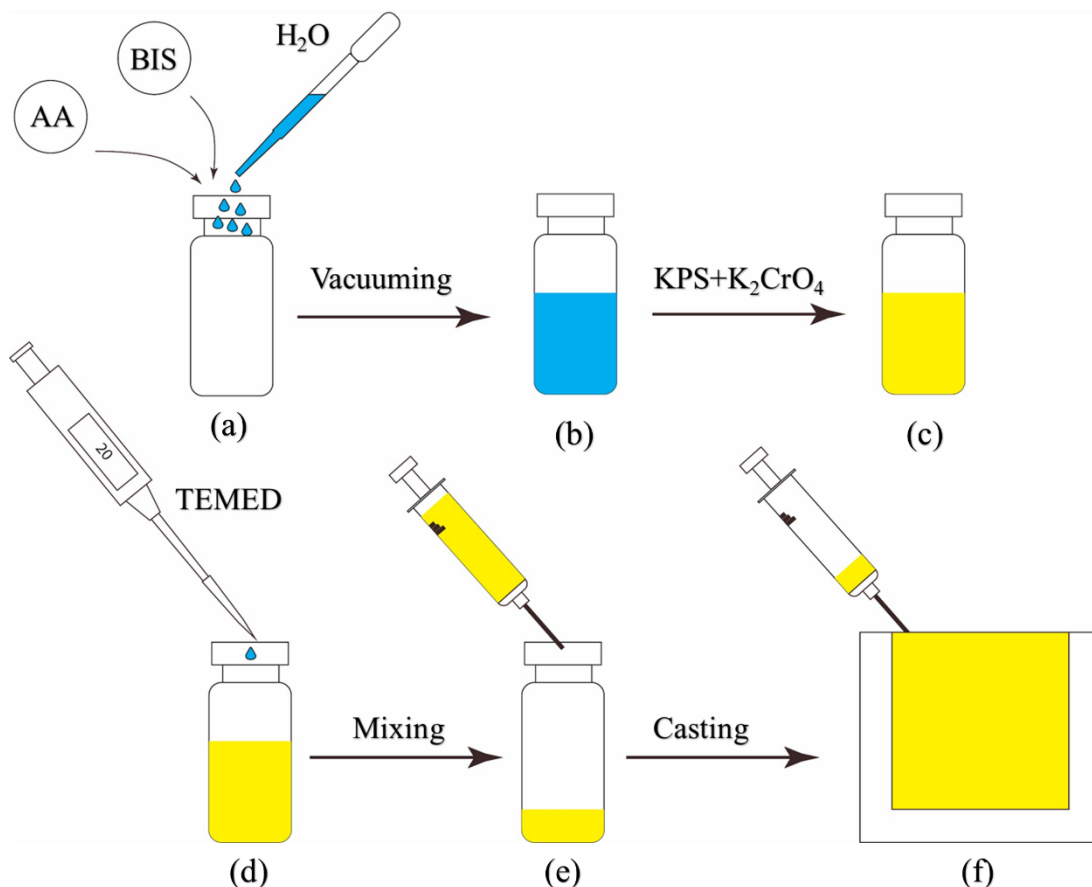


Figure 9. Preparation and cast molding of polyacrylamide (PAA) hydrogel. (a) Acrylamide (AA) and Bis-acrylamide (BIS) are dissolved in deionized water. (b) Solution is degassed under vacuum for 20 minutes. (c) KPS and  $K_2CrO_4$  are added and mixed carefully to the solution not to introduce further oxygen in the sample. (d) Addition of TEMED and gelation initiation in prepared solution after addition of TEMED. (e and f) Casting of solution in plexiglass mold before first gelation stage complete using syringe.

### 2.3. Preparation of polyacrylamide (PAA) hydrogels with secondarily-added potassium chromate content

1.446 g acrylamide (AA) and 0.002 g Bis-acrylamide (BIS) were dissolved in 9.2 ml deionized water. The solution was degassed in vacuum for 20 minutes. 0.02 g of potassium peroxydisulfate was added and mixed carefully not to introduce further oxygen in the sample. Immediately after addition and mixing of 20  $\mu$ L TEMED, prepared hydrogels were casted in the plexiglass molds. Samples were stored in room temperature for 24 hrs. for complete gelation to occur. Afterward, samples were

removed from the mold and were dried in 70 °C for 12 hours. Dried gels were dipped and swelled in 9.2 ml of deionized water containing 0.02 g (0.01 M) of potassium chromate for 24 hours.

#### 2.4. Preparation of 3D polyacrylamide-sodium alginate hybrid hydrogel

For preparation of **3D** hybrid hydrogels of polyacrylamide-sodium alginate hydrogels, polyacrylamide precursors were scaled 6 times the conventional amount with the same weight concentration (section 2.2) in deionized water. Accordingly, 8.676 g acrylamide (AA), 0.036 g Bis-acrylamide (BIS), 0.12 g of potassium peroxydisulfate (KPS) and 0.12 g of potassium chromate were dissolved in 25.2 ml deionized water (solution 1). 0.15 g of sodium alginate was separately dissolved in 30 ml of water in ice bath (solution 2). The solutions were mixed and degassed in vacuum for 20 minutes. 120  $\mu$ L TEMED was added and samples were casted in polystyrene (PS No. 6) cuboid molds (4 cm  $\times$  4 cm  $\times$  4 cm) to form **3D** hydrogels.

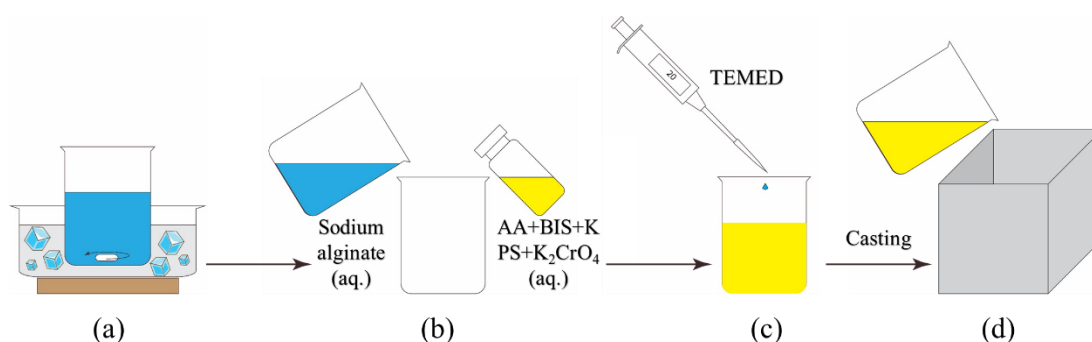


Figure 10. Preparation of the **3D** polyacrylamide-sodium alginate hybrid hydrogel. (a) Dissolving 0.15 g sodium alginate (SA) in 30 ml deionized water in ice bath. (b) Mixing sodium alginate solution and polyacrylamide (PAA) hydrogel precursors (8.676 g acrylamide (AA), 0.036 g Bis-acrylamide (BIS), 0.12 g of potassium peroxydisulfate (KPS) and 0.12 g K<sub>2</sub>CrO<sub>4</sub>) dissolved in 25.2 ml deionized water. (c) Addition of 120  $\mu$ L TEMED as catalyst to start gelation. (d) Pouring solution to polystyrene (PS No. 6) cuboid molds (4 cm  $\times$  4 cm  $\times$  4 cm).

#### 2.5. Preparation of the 3D agarose gels

3.2 g agarose was mixed in 36.8 ml deionized water to yield a 8 w% agarose solution. Two different types of samples were prepared; one containing 0.01 M K<sub>2</sub>CrO<sub>4</sub> as inner

electrolyte and in the other 0.01 M  $\text{CuCl}_2$  as inner electrolyte dissolved in agarose-water mixture. For both, agarose mixture was taken into a glass beaker and was covered with a stretch-film to avoid splashing of the melt upon Microwave heating, which was continued until all agarose melts. The melt was cast-molded in a spherical mold of a Ping-Pong ball with 40 mm diameter. (The mold was prepared by cutting ping pong ball into two halves. Then, two halves were taped together and a hole was punched to provide a path for the cast to be injected.) Casted sample was left to cool in refrigerator and solidify. After 1 hour in the refrigerator, the sample was demolded for the experiment. The sample containing potassium chromate sample was dipped in 1 M  $\text{CuCl}_2$  solution and the sample with  $\text{CuCl}_2$  was dipped in 1 M  $\text{K}_2\text{CrO}_4$  solution for 24 hours.

## **2.6. Preparation of the agarose stamp**

For stamp preparation 0.80 g agarose was added to 9.2 ml deionized water. This mixture was heated in microwave until agarose melts. The agarose melt was molded in **3D** printed (Zortrax, M200) cylindrical (for **2D** setup) and cuboid (for **1D** setup) polylactic acid (PLA) mold (cylindrical: diameter = 1 cm, height = 0.8 cm; cuboid: 1 cm  $\times$  1.5 cm  $\times$  1 cm). Samples were left for 20 minutes in the refrigerator to solidify. Prepared stamps were dipped in 1.0 M  $\text{CuCl}_2$  solution as outer electrolyte (unless otherwise is mentioned) for 40 minutes.

## **2.7. Preparation of the Ecoflex substrate**

A homogenous mixture of 50 %w Ecoflex A, and 50 w% Ecoflex B was prepared by vigorous mixing and the mixture was poured into a Plexiglas mold. The mixture was let to stay in the mold until all bubbles were removed (ca. 5 min). 2 wooden sticks (thickness = 2 mm), which served as a solid surface that polyacrylamide hydrogel can later stick onto, were placed gently on the uncured Ecoflex. (The top surface of sticks should not be covered with Ecoflex.) Ecoflex-wood composite was cured in oven at 60 °C for 45 minutes.

## 2.8. The experimental setup for mechanical deformation in 1D and 2D gels

Figure 11 illustrates the setup and procedure for deforming (stretching/releasing) hydrogels with **2D** Liesegang patterns in PAA hydrogel. Prepared PAA hydrogel (section 2.2) was removed from the mold and was transferred on Ecoflex substrate (as mentioned in section 2.7). To apply load on the hydrogel sample (stretching), we used an Ecoflex substrate, on which the gel was placed. Direct attachment of hydrogel to the holders without the Ecoflex substrate would break the hydrogel at the clamp jaws due to a high load of perpendicular forces. Then, the stamp (2.6) was placed gently on the hydrogel center as described in the individual experiments.

**1D** stretching setup was prepared similar to the **2D** setup; using (1.5 cm × 7 cm × 2 mm) hydrogels and the cuboid stamp was placed on the hydrogel center. All samples were kept in a container, in which water was sprayed to cease evaporation of water from the hydrogel and the stamp during the experiments.

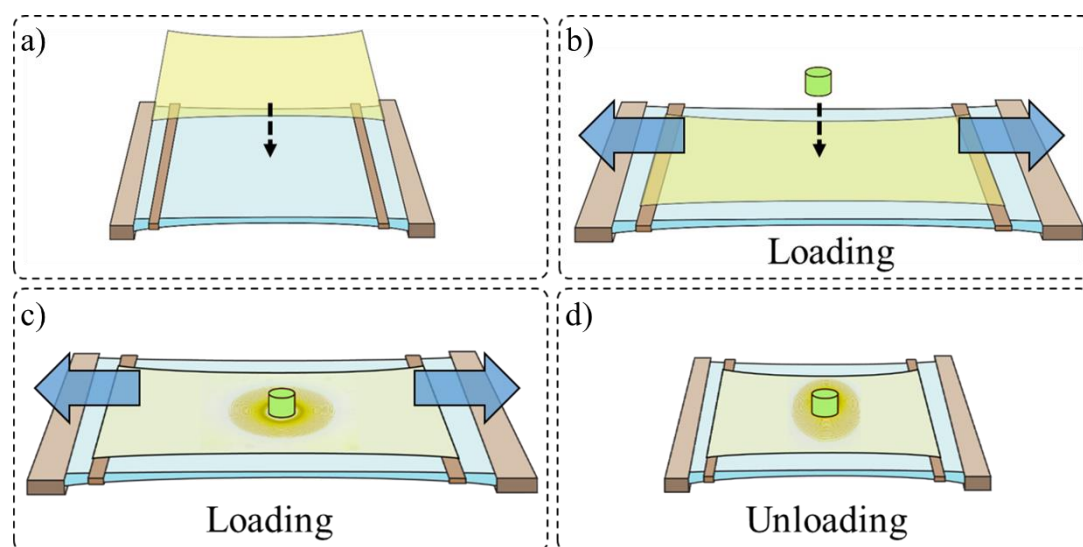


Figure 11. Schematic illustration of **2D** uniaxial stretching setup. (a) Transferring hydrogel on Ecoflex substrate. (b) Loading (stretching) sample, followed by stamp placing at the center of the hydrogel. (c) Formation of the patterns on the hydrogel upon loading. (d) The sample unloading.

## 2.9. Chemical erasing of the LPs formed in the hydrogels

Precipitation patterns formed on PAA hydrogels were removed using three different solutions. Hydrogels with patterns were dipped in 20 ml of 0.1 M HCl, acetic acid, and NH<sub>3</sub> solutions and were left in the solutions for 2 hours.

## 2.10. Polymerization of pyrrole on LP patterns

1 ml of 0.1 M HCl was added to 28.8 ml of deionized water. Then, 0.2 ml of Pyrrole solution was added to this solution. The mixture was sonicated and shaken vigorously to dissolve pyrrole emulsions in water completely. The hydrogels were directly dipped in this solution/emulsion and kept in them until the development of the polypyrrole on the LP patterns [54].

## 2.11. Optical imaging

Images were captured using a Canon EOS Rebel T2i with a Canon EF 50 mm f/2.5 Macro Lens. Samples were illuminated using bottom-illuminated LED light box.

## 2.12. Image processing and analysis

Data was extracted using ImageJ software. Figure 12a shows an example of LPs characterization using Gray-value (brightness of a pixel, in the range of 0 to 255 in ImageJ software; gray-value = 0.299red + 0.587green + 0.114blue). In Figure 12b, gray-values of an LP is shown. Data collected using ImageJ (ImageJ can produce a linear profile of the grayscale values of the image pixels.) was processed in MATLAB using a self-written MATLAB code exploiting “Findpeaks” function, to find the peaks intensity, position, width and *prominence* (difference between gray-value of bands and their neighbor depletion zone). Spacing coefficient of patterns signal ( $X_{n+1}/X_n = 1 + p$ ) was retrieved from the slope of  $\ln(X_n)$  vs.  $n$ , where  $X_n$  is the position of each precipitation band and  $n$  is the band number and  $\ln(X_n)/n = \ln(1 + p)$ . Width of bands was retrieved by calculating full width at half maximum of negative of gray-value ( $-1 \times$  gray-value).



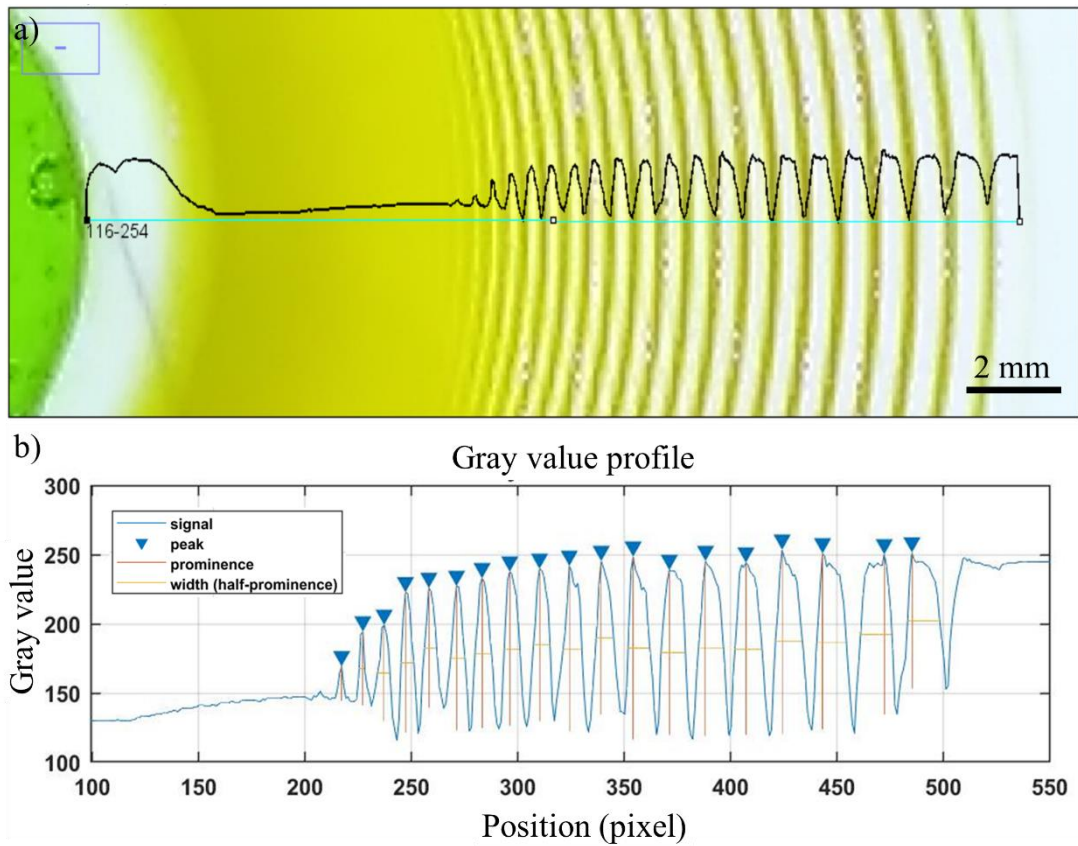


Figure 12. Gray-value analysis of Liesegang patterns in Figure 13a. (a) Gray-value profile of LPs in loading (stretching) direction just before unloading. (b) Peaks analysis of gray-value profile including peak intensities, widths (full width at half maximum) and peak *prominences* (difference between gray-value of bands and their neighbor depletion zone).

## CHAPTER 3

### 3. RESULTS AND DISCUSSION

#### 3.1. Formation of post-patterns in 1D, 2D, and 3D PAA hydrogels

##### 3.1.1 Formation of post-patterns in 2D PAA hydrogels

The changes in the LP patterns affected by elastic mechanical deformation of the gels shown so far are 1) the alteration of the aspect ratio of the whole pattern by the deformation, 2) the formation of the post-patterns (PP) upon the continuing reaction/diffusion after the unloading. In this section, we would like to concentrate more on the latter phenomenon, the formation of the post-patterns, since they are more information-rich. Post-patterns (PP) stand out as irregularities in the reaction-diffusion system as a result of previously experienced mechanical input. They can be detected visually, which make them suitable for further analysis without utilization of any special technique. In Figure 13, the formation of PPs in a stretched polyacrylamide gel, where  $\text{CuCrO}_4$  precipitation patterns form, is shown. Firstly, the stretchable polyacrylamide gel was deformed uniaxially and elastically (Figure 13a) for 24 hrs. During this time  $\text{Cu}^{2+}$  ions from the agarose stamp diffused into the hydrogel and the LP patterns formed as expected, as concentric circular rings (aspect ratio =1.0) around the stamp, following the LP spacing and width laws. (As mentioned above, spacing law (spacing coefficient:  $1 + p = X_{n+1}/X_n$ ) is one of the governing laws in LPs, which means that spacings between the consecutive pattern bands form a mathematical geometric series.) After releasing the load, the LP pattern adopted an aspect ratio higher than 1.0 (as also shown in Figure 6). Note that in the unloaded gel, even though the formed LPs were distorted because of the unloading, to concentric ovals, they still follow the ‘LP laws’. If the reaction/diffusion is let to continue after

this point, the PPs start to develop, which have distinct characteristics: 1) the intra-ring depletion zone (the space between the consecutive rings, where there is no significant precipitation detected in regular LPs) has a darker color, 2) in this region, PPs deviate from the LP-spacing-law; a few consecutive bands form as equidistant rings. Figure 13 also shows a ‘recovery’ of the reaction-diffusion system - after formation of a couple of PPs, the system reverts back to forming regular LPs.

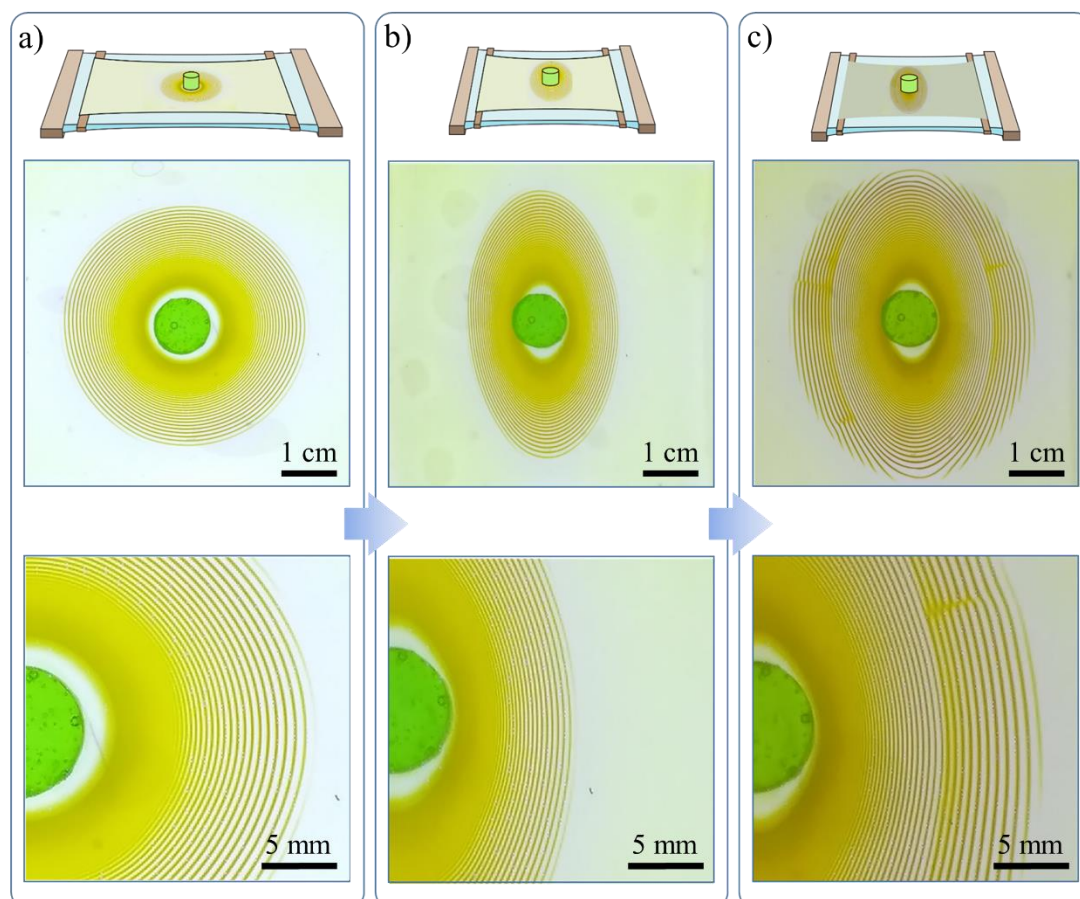


Figure 13. A typical demonstration of PP formation in **2D** hydrogel. (a-c) The patterns of  $\text{CuCrO}_4$  formed by diffusion of  $\text{Cu}^{2+}$  into  $\text{CrO}_4^{2-}$  containing polyacrylamide (PAA) gel during and after elastic deformation of the gel. (a) Formation of patterns in a stretched (40% strain) PAA hydrogel after 24 hours. (b) The change in the aspect ratio of patterns after unloading (releasing) the stress. (c) Post-patterns formed in the sample after unloading (release) (photo taken 18 hours after unloading). *Inner electrolyte (potassium chromate) = 0.01 M, outer electrolyte (copper chloride) = 1 M, acrylamide = 13.5 w%, BIS = 0.056 w%, KPS = 0.187 w%, TEMED = 0.0001 w%.  $T = 20\text{ }^\circ\text{C}$ .*

*For details of the gel preparation and loading setup please see Chapter 2.*

To document the formation of the PP, we preferred to utilize gray-value measurements, which is available in ImageJ software [55]. As can be seen in Figure 14, in a typical **2D** sample, gray-value profile which is overlaid on to the optical image of the patterns, clearly shows the difference between the LPs and PPs formed.

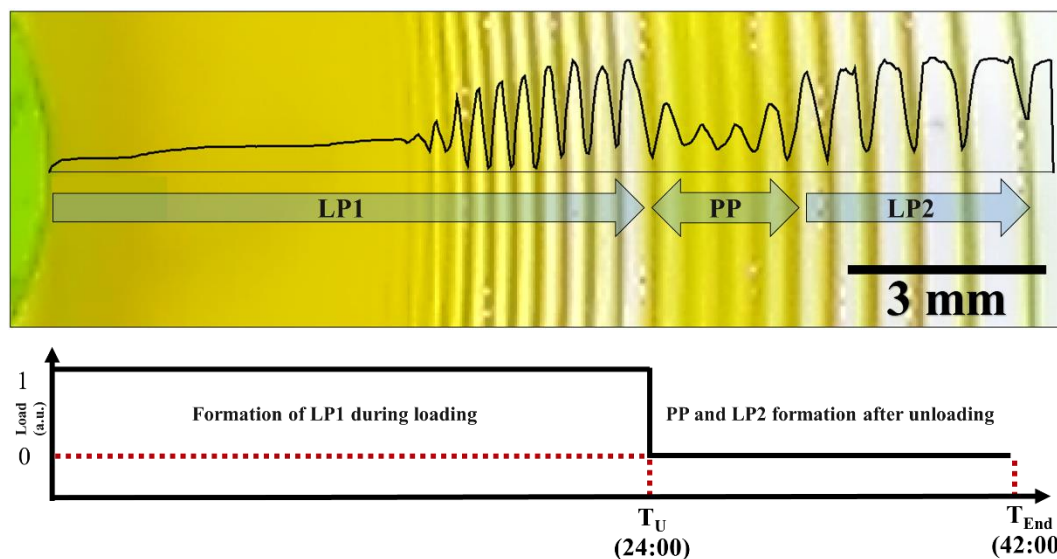


Figure 14. Gray-value profile of the patterns of  $\text{CuCrO}_4$  formed by diffusion of  $\text{Cu}^{2+}$  (1 M) into  $\text{CrO}_4^{2-}$  (0.01 M) containing polyacrylamide gel during and after elastic deformation of the gel (close-up of the patterns in loading (stretching) direction in Figure 13c). During the 24-hour loading, regular LP1 form. Post-pattern (PP) and LP2 regions form after unloading (releasing) the sample (18<sup>th</sup> hour after unloading). *Inner electrolyte (potassium chromate) = 0.01 M, outer electrolyte (copper chloride) = 1 M, acrylamide = 13.5 w%, BIS = 0.056 w%, KPS = 0.187 w%, TEMED = 0.0001 w%.  $T = 20^\circ\text{C}$ . 40 % strain upon loading for 24 hrs. Photo taken in 18 hours after unloading. For details of the gel preparation and loading setup please see Chapter 2.*

The differences in the LP and PP patterns that can already be detected visually, can be made more distinct by means of image analysis. Gray-value analysis of patterns (Figure 15) was performed using a self-developed MATLAB code, which generates a gray-value plot of the image pixels with respect to the distance from the stamp. From the gray-value profile, the position of bands in the patterns was retrieved as the peak maxima, which was later used to calculate the spacing coefficients between the consecutive bands. Also, the band width can be expressed as the full width at half maximum of the peaks. The intensities of the peaks were used, too, in order to compare

the sharpness of the patterns formed, and to differentiate between LPs and PPs (Figure 15b-e). The results summarized in Figure 15 shows that there are three different regions in the precipitation profile. The first region, labelled as *LP1*, which forms under mechanical deformation, consists of ordinary LPs. The second region is formed by a couple of irregular post-pattern (PP) bands, which are due to the precipitations after unloading. After formation of a couple of *PP* bands, precipitation patterns start to self-regulate themselves and regular LPs start to form again (*LP2*). The details of the pattern differences in these three regions can be summarized as follows. The sharp color contrast between the LP bands and the light-colored background that is observed in the cases with regular LPs decreases drastically when the system starts to form the PP patterns (as seen from the reduced peaks prominences). (gray-value contrast between the precipitation band and the depletion zone changes from 100 to 50 (in the scale of 0 to 255) which shows 50% change in contrast.) In addition, the gray-value analysis clearly quantifies the spacings between the rings, and shows that the patterns formed after unloading (PP) do not follow the spacing law of the regular LPs Figure 15c). Similarly, width law is also not obeyed upon PP formation (Figure 15b), however, it is more difficult to quantify this, due to the errors [56] emerging from the gray-value analysis, upon the determination of the full width at half maximum of the gray-value peaks.

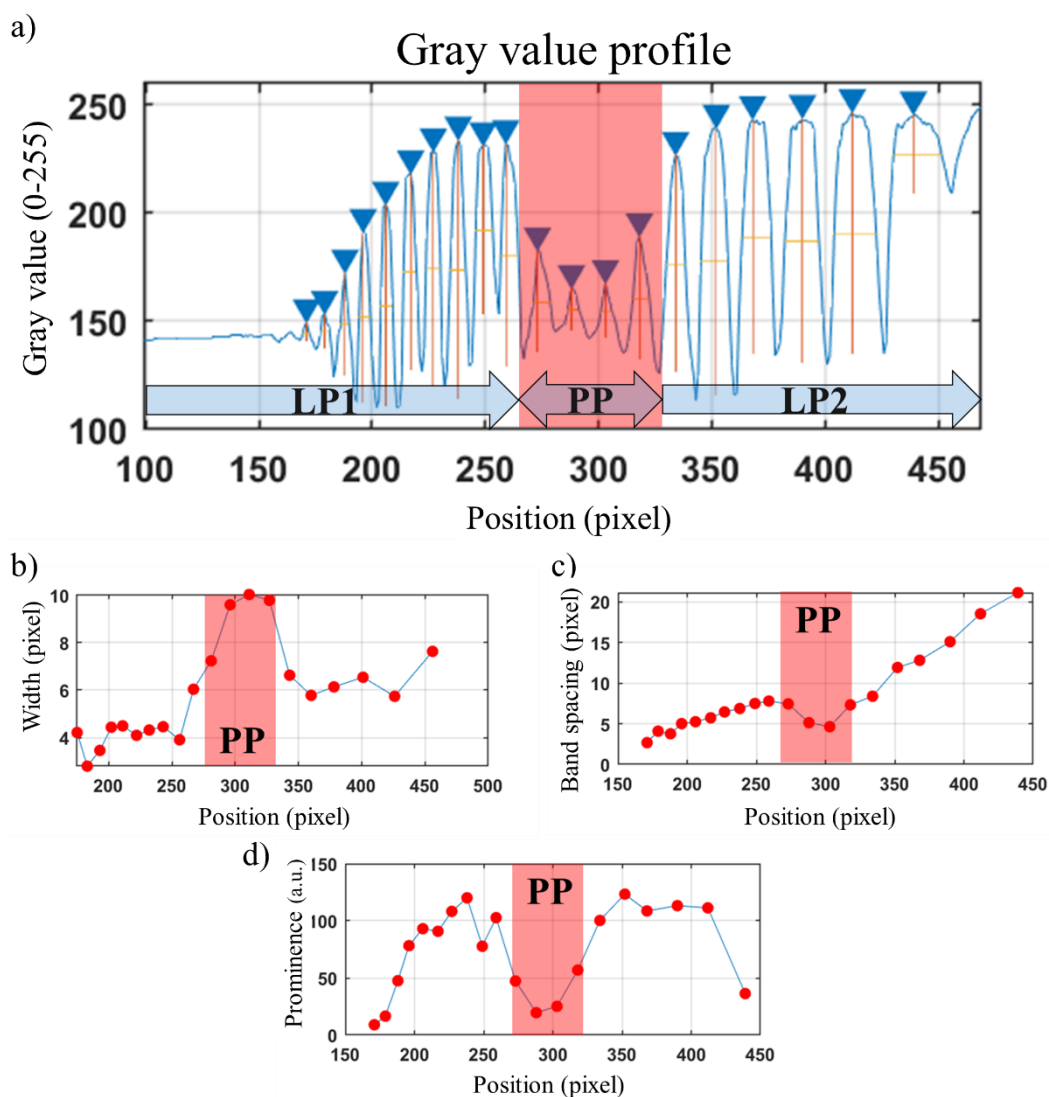


Figure 15. Differences between the patterns formed after unloading (PP) and the regular LP formed during loading (LP1) and long after unloading (LP2). (a) Gray-value analyses of the patterns of  $\text{CuCrO}_4$  formed by diffusion of  $\text{Cu}^{2+}$  (1 M) into  $\text{CrO}_4^{2-}$  (0.01 M) containing polyacrylamide gel during and after elastic deformation of the gel (data retrieved from the gray-value analysis of the image shown in Figure 14). Changes in (b) the width of patterns, (c) the spacing of the two consecutive bands, (d) the peak prominence (difference between gray-value of bands and their neighbor depletion zone).

Our results, as illustrated in Figure 16, show that post-pattern formation is not just limited to loading-unloading (LU) event, but it can also be observed in unloading-loading event (UL), or unloading-loading-unloading cycles (ULU). (Figure 16).

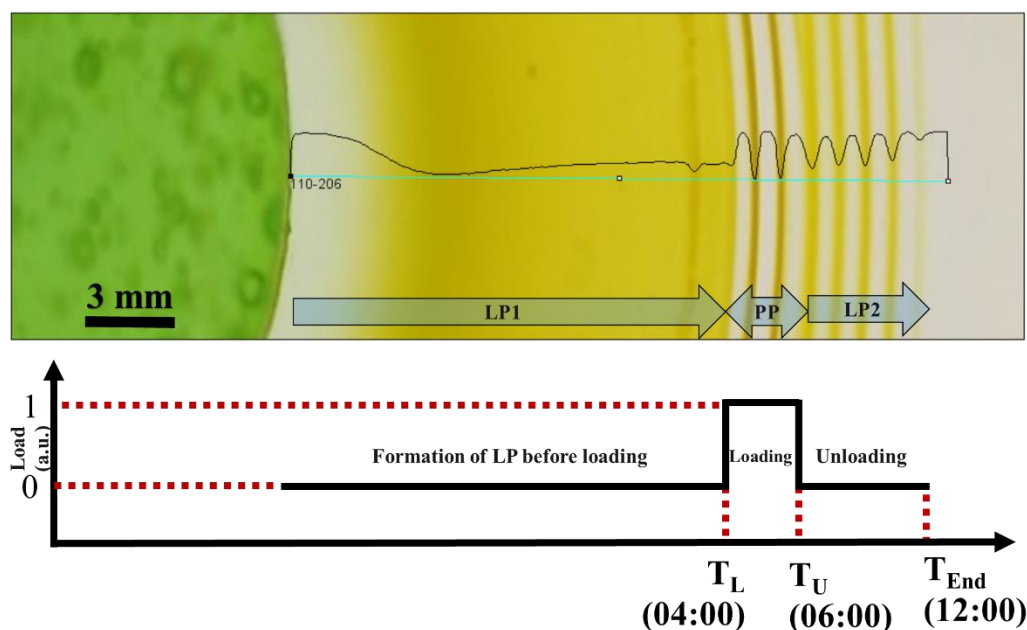


Figure 16. Gray-value profile of precipitation patterns upon loading at the 4th hour and unloading at the 6th hour. Stamp is placed on an unloaded polyacrylamide (PAA) hydrogel. After 4 hours of LP formation, the sample is loaded (stretched) up to 40 % strain. PPs and LP2s are led to develop, then sample is unloaded after 2 hours and the photo is taken after 6 hours. *Inner electrolyte (potassium chromate) = 0.01 M, outer electrolyte (copper chloride) = 1 M, acrylamide = 13.5 w%, BIS = 0.056 w%, KPS = 0.187 w%, TEMED = 0.0001 w%. T = 20 °C. For details of the gel preparation and the loading setup please see Chapter 2.*

In the UL event, while patterns are forming, the PP formed during loading form with distinctly higher spacings between the consecutive rings. In contrast to PPs in LU event, in the UL event causes the intra-band region or ‘the depletion zone’ (the area between the bands, where the precipitation is at its minimum) to become lighter and the color contrast between the pattern bands and the depletion zone increases. This can be displayed comparing the peaks prominences (difference between the gray-value of peaks and those in their neighbor depletion zone), and also tracking the evolution of new bands: a depletion zone with a width of 13.5 is observed right after a precipitation

band with a width of 8.33 pixel. PP bands can be distinguished with their prominence of 92 following by LP with prominences of ca. 66 with 28 % decrease) (Figure 17b).

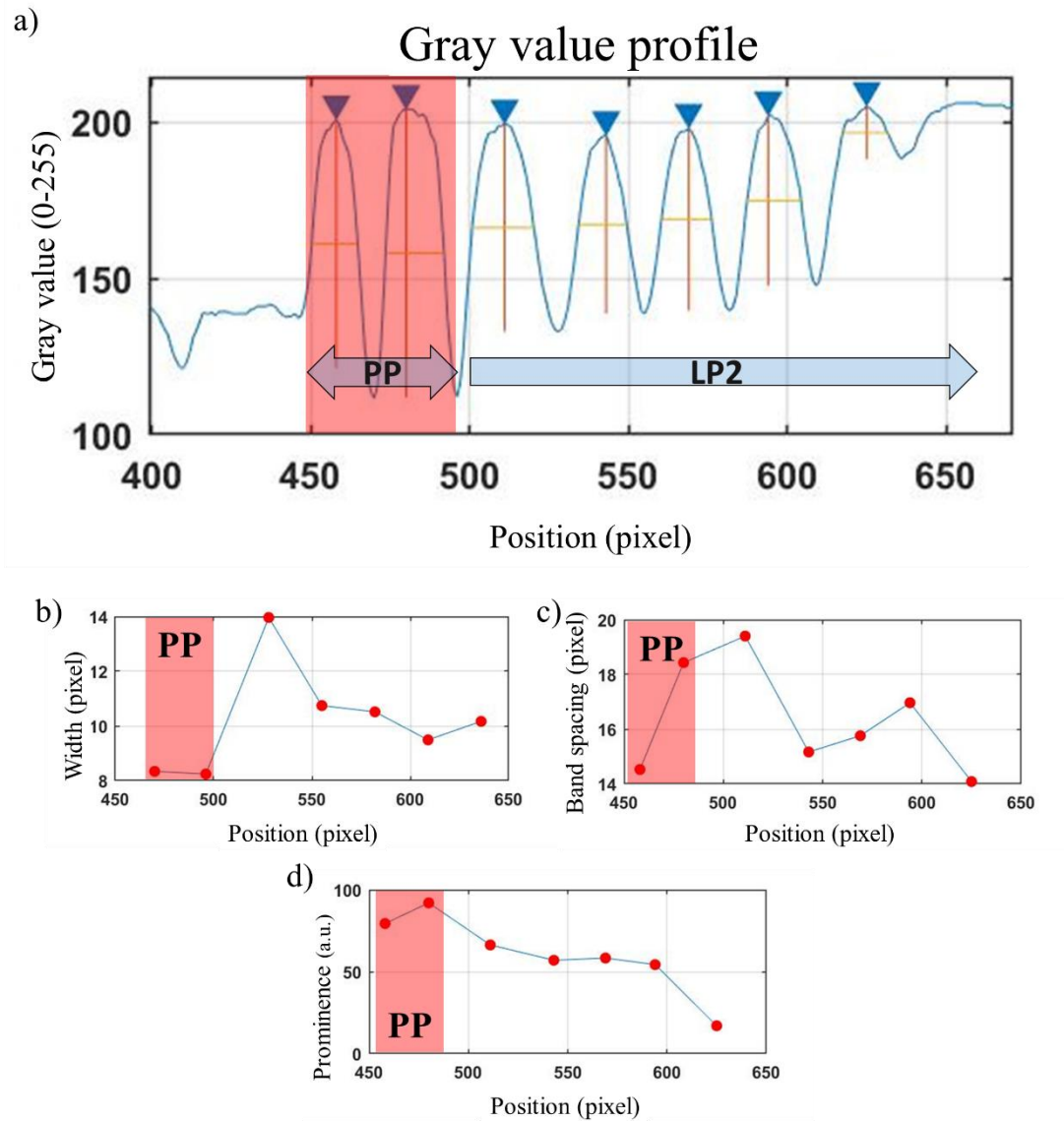


Figure 17. Gray-value analyses of the PP and LP2 displayed in Figure 16. (a) Gray-value profile. Changes in (b) the width of patterns, (c) the spacing of the two consecutive bands, (d) the peak prominence (difference between gray-value of bands and their neighbor depletion zone). (here, LP1 are not shown since their line spacings are too small to be detected by gray-value analyses))

### 3.1.2 Formation of post-patterns in 1D PAA hydrogels

Since **2D** samples are harder to prepare and to model, the most straightforward setup to analyze the formation of the post-patterns, which is a **1D** system, is adopted for



developing a mathematical model on the system (Figure 22). In the one dimensional system, parallel bands of precipitation form, rather than concentric rings of the **2D** system, which makes the analysis, that uses spacings of the bands, much easier. In practice, **1D** system is just different from the **2D** that a cuboid stamp is used, which has a length the same as the hydrogel width (Figure 18).

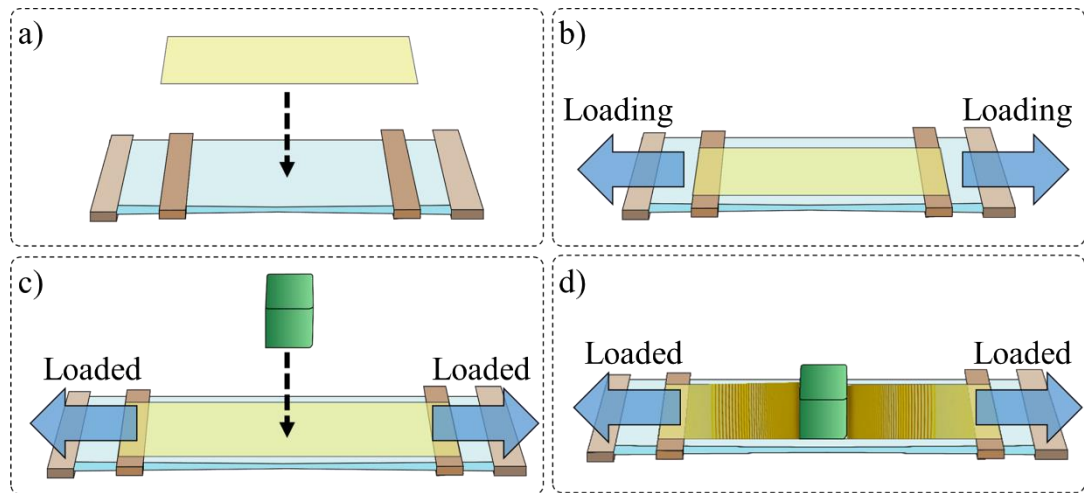


Figure 18. Schematic illustration of the steps involved in the preparation of the setup for **1D** Liesegang pattern formation. (a) Placing polyacrylamide (PAA) hydrogel on Ecoflex substrate. (b) Loading and stretching PAA hydrogel. (c) Placing cuboid stamp at the center of the PAA hydrogel. (d) **1D** Liesegang patterns forms as parallel bands. Note that the length of the stamp should be the same as the hydrogel width to obtain these parallel precipitation patterns.

In the preliminary experiments, to examine the consistency of the pattern formation in this new, **1D** configuration, we started by investigating the pattern formation in agarose hydrogels. Agarose is the conventional medium for production of LPs in the literature. After the successful formation of  $\text{CuCrO}_4$  LPs in agarose with the same inner and outer electrolyte concentration as used in our **2D** PAA system (section 2.2), we switched the gel medium to stretchable gel, PAA. As shown in Figure 19, in PAA, too, LP can form, although the bands are closer to the stamp because of the differences of diffusion coefficients of the electrolyte ions in the new gel medium, PAA. As expected from the similar observation with the **2D** samples (section 3.1.1); a uniaxial tensile elastic deformation of the gel results in the development of the patterns in the loaded state that are identical to the ones developing in the control sample (Figure 19f-g), since the mechanical deformation of the gel does not affect the

diffusion coefficient of the electrolyte (see also, Figure 6). Upon unloading, however, the pattern ‘shrinks’ in the reverse direction of the previous tension, as shown in Figure 19d. At this point, if the patterns are allowed to develop further, they form the PPs, again, similar to the case with **2D** gels, Figure 19e. In contrast to ‘secondary rings’ reported by Smoukov et al. [30], formation of the post-patterns is not limited to **2D** geometry and can appear in **1D** as well.

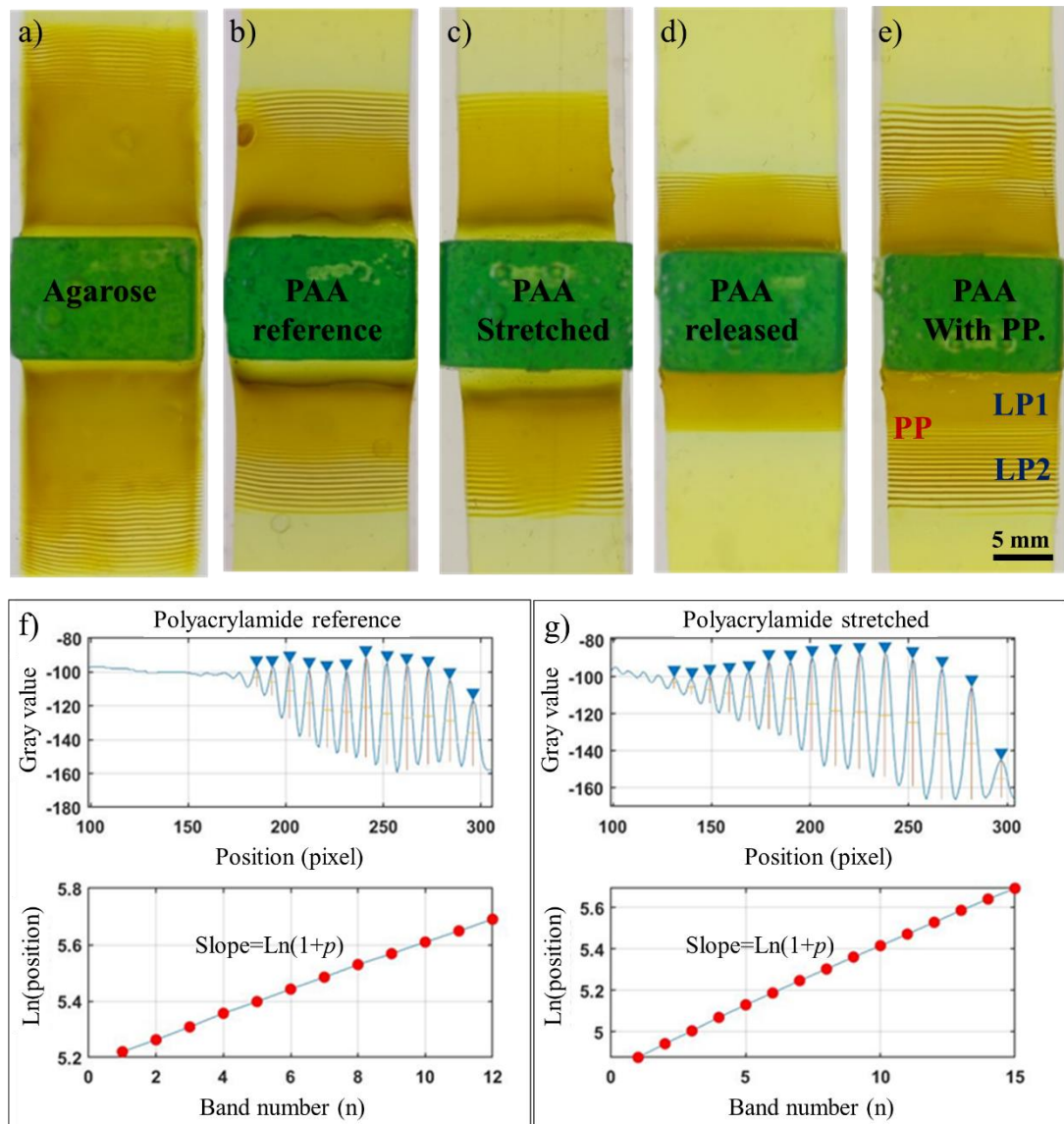


Figure 19. The formation of precipitation patterns in **1D** gels, the effect of uniaxial, tensile elastic deformation on the pattern formation in the polyacrylamide (PAA) gel. (a) Formation of LPs in Agarose (Agarose, 8 w%). (b) LPs formed in a reference (unloaded) PAA hydrogel (*acrylamide* = 13.5 w%, *BIS* = 0.056 w%, *KPS* = 0.187 w%, *TEMED* = 0.0001 w%.  $T = 20\text{ }^{\circ}\text{C}$ ) after 12 hours. (c) LPs formed in the loaded (40%

strain) PAA sample after 12 hours. (d) ‘Shrinking’ of LPs in the reverse direction of the previous tension in the PAA just after unloading. (e) Formation of PPs and LP2s in PAA hydrogel after unloading, in 12 hours. (f-g) Gray-value profiles of LPs developed in the reference and the loaded PAA gel after 12 hours of loading. *In both Agarose and PAA hydrogels: Inner electrolyte (potassium chromate) = 0.01 M, outer electrolyte (copper chloride) = 1 M. For details of the gel preparation and the loading setup please see Chapter 2.*

The elastic mechanical deformation can mathematically be described in the form of ‘stretching’ and ‘compressing’ functions (Figure 20). In this mathematical approach based on the extent of strain, the resulting geometry of hydrogel after deformation in one dimensional configuration can be written in the form of:

$$f(x_{new}) = f\left(\frac{1}{1-\varepsilon}x\right) \quad (3-1)$$

where  $\varepsilon$  is strain due to mechanical deformation. This way we can rewrite new equations ((1-1)~(1-4)) by just changing Fick’s second law of diffusion and knowing that concentration ( $c$ ) at any specific time is a function of position:

$$c(x_{new}) = c\left(\frac{1}{1-\varepsilon}x\right) \quad (3-2)$$

$$\nabla_x^2 c(x_{new}) = \left(\frac{1}{1-\varepsilon}\right)^2 D \nabla_x^2 c_x \quad (3-3)$$

Such consideration can be useful for numerical solution of partial differential equations (PDE) sets of Liesegang system.

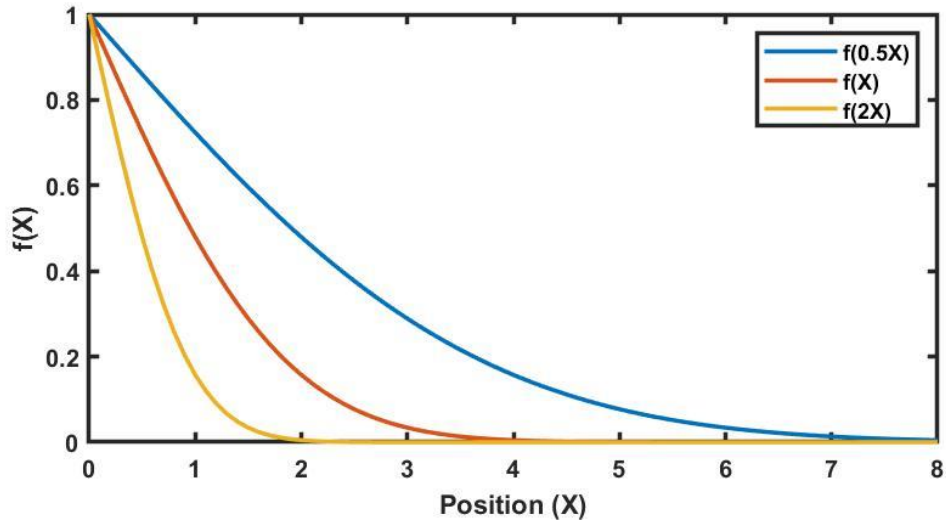


Figure 20. Demonstration of the stretching and the compressing functions. Elastic mechanical deformation can be explained mathematically using so called stretching and compressing functions. If  $f(x)$  represent (red) concentration profile in a medium,  $f(0.5x)$  represents (yellow) the concentration profile in the case of ‘shrinkage’ with -50% strain (can be analogue to stretched/released transformation) and  $f(2x)$  shows (blue) concentration profile upon stretching the sample with 50% strain (unstretched/stretched transition).

In **1D** system, it is also quite straightforward to visually find the position of the diffusion fronts, which give information about the mechanical strain (Figure 19e). In Figure 21, the deformation of PAA hydrogels with different extent of strains (10 %, 20 %, 30 %, 40% and 50%) can be seen after loading for 12 hrs (the formation of LP1), unloading and waiting for 12 hrs, additionally (the formation of PP and LP2). Diffusion front (position labelled by red arrow) just before the formation of the post-pattern region is revealing the extent of deformation that the sample has endured. The higher the strain on the sample, the closer appears this front to the stamp. Also, by increasing the extent of deformation (from 10 to 50 % strain) the position of post-patterns, their number, and width are found to be different. It can be said that the higher the strain, the closer is the post-pattern region to stamp and broader the PPs region.

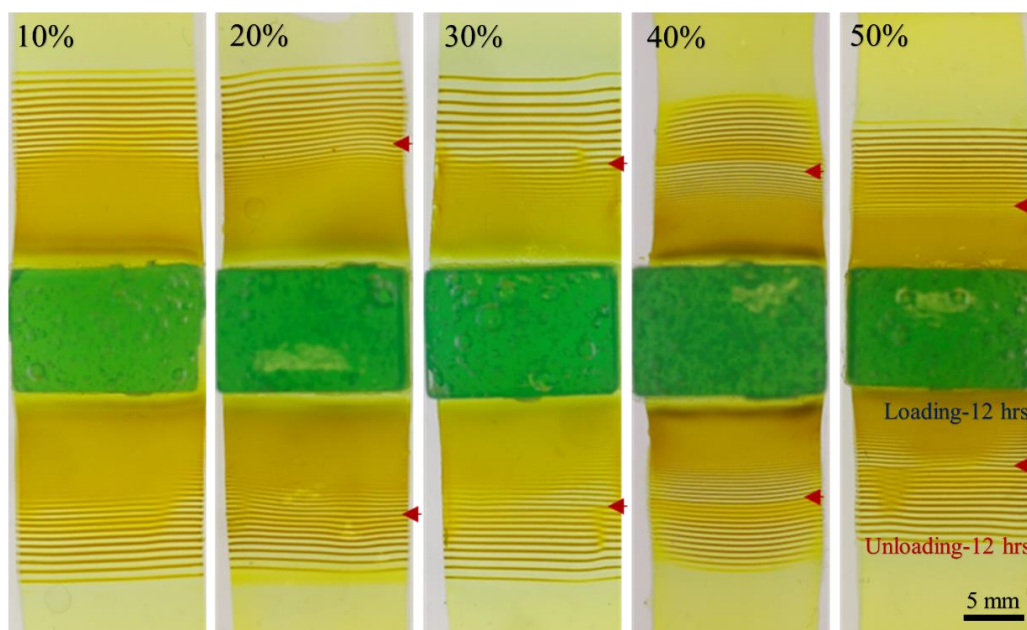


Figure 21. The formation of PP in **1D** polyacrylamide (PAA) gels loaded to 10-50% strain. LP formed during 12 hours of loading; after unloading, 12 hours of waiting generates PP and LP2. *Inner electrolyte (potassium chromate) = 0.01 M, outer electrolyte (copper chloride) = 1 M, acrylamide = 13.5 w%, BIS = 0.056 w%, KPS = 0.187 w%, TEMED = 0.0001 w%. T = 20 °C. For details of the gel preparation and loading setup please see Chapter 2.*

Another important point to emphasize here is that both PP and LPs are retained in the overall pattern as they are formed in the course of time. Figure 22 shows the time evolution of LPs and PPs in a PAA gel with 40 % strain upon loading – the images taken every 30 mins after the unloading show that only new bands are added with time, the ‘old bands’ do not move or develop.

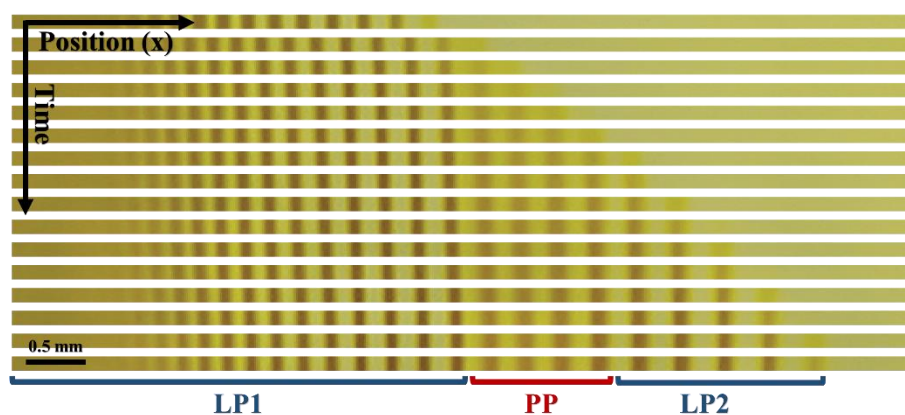


Figure 22. Time evolution of the precipitation patterns in a **1D** PAA gel with LP1s already developed (Figure 21d). LP formed for 12 hours and the consecutive photos

are showing time evolution of pattern formation (PPs and LPs) after unloading the stress. The patterns were developed for further 8 hours, images were taken every 30 minutes. *For details of the gel preparation and loading setup please see Chapter 2.*

### 3.1.3 Formation of LP and post-patterns in 3D hydrogels

#### 3.1.3.1 Formation of post-patterns in 3D agarose gels

To study formation of LP patterns in **3D**, we started with agarose as the medium. Two different types of samples were prepared; in the first one,  $\text{K}_2\text{CrO}_4$  (0.01 M) was doped into agarose hydrogel as the inner electrolyte, and the sample was left in  $\text{CuCl}_2$  (1 M) solution surrounding the sphere. In this sample no precipitation pattern was observed. In the second sample, in which  $\text{CuCl}_2$  (0.01 M) served as the inner electrolyte and  $\text{K}_2\text{CrO}_4$  as outer electrolyte (1 M), very irregular but visible patterns were formed which can be seen in Figure 23.

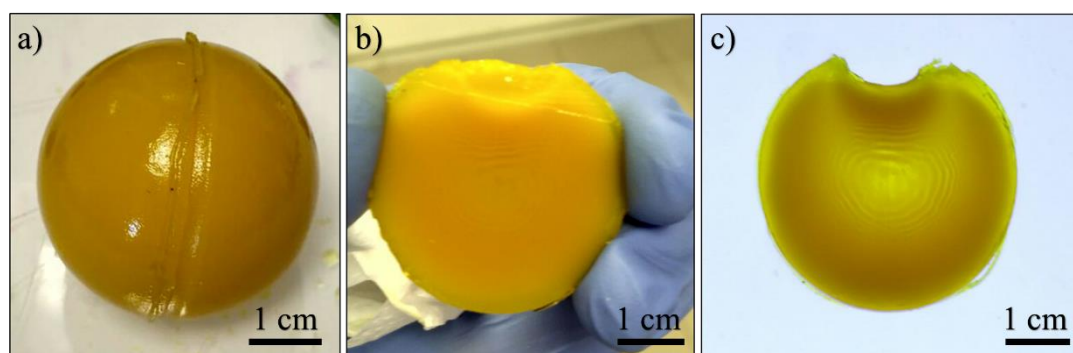


Figure 23. Formation of precipitation patterns in **3D** in 8 w% agarose sphere. (a) Agarose sphere removed from 1 M  $\text{K}_2\text{CrO}_4$  outer electrolyte solution. (b) Cross section of **3D** sample. (c) Thin layer cut from sample for rings detection. *Inner electrolyte (copper chloride) = 0.01 M, outer electrolyte (potassium chromate) = 1 M,  $T=20$  °C. For details of the gel preparation please see Chapter 2.*

Although the formation of precipitation patterns in **3D** gels are observed through the second configuration (*vide supra*), this method does not provide clean, sharp and distinctive patterns that is needed for further study. For better preparation of **3D** samples to display PP formation, we worked on an agarose hemisphere we prepared, containing 0.01 M  $\text{K}_2\text{CrO}_4$  as inner electrolyte, and placed an stamp (agarose = 8 w%) providing 1 M  $\text{CuCl}_2$  as outer electrolyte on the equatorial plane of the hemisphere gel for 24 hours similar to the wet stamping of **2D** gels, Figure 24.

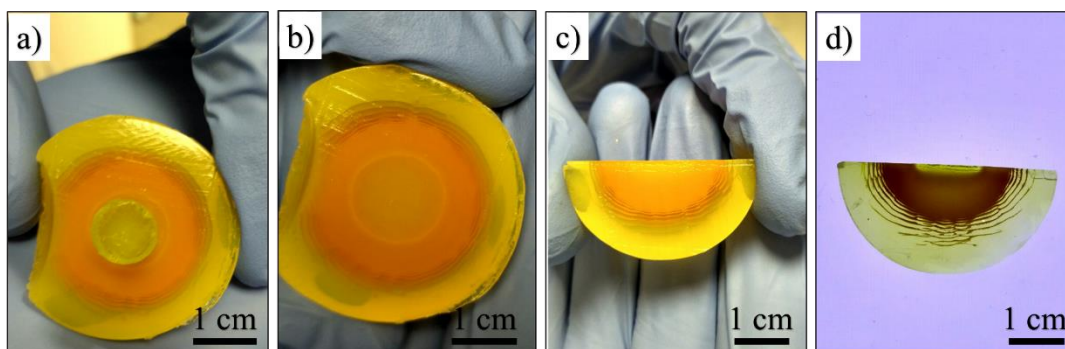


Figure 24. The formation of **3D** patterns in an agarose hydrogel hemisphere (diameter = 4 cm) using wet stamping method. (a) Patterns formed after 24 hours. (b) Top view of sample without stamp. (c) Cross section of sample after cutting to halves. (d) Thin film cut of cross section for rings detection. *Inner electrolyte (potassium chromate) = 0.01 M, outer electrolyte (copper chloride) = 1 M. T = 20 °C. For details of the gel preparation please see Chapter 2.*

In **3D** samples, compression of the gel is practically easier than applying tension to the gel, so we adapt the system to the compression setup. Since the hemisphere gel described above was not ideal for homogeneous mechanical input, we switched to a cubic agarose gel sample with 4 cm X 4 cm X 4 cm dimensions. For applying the deformation, the cubic hydrogel was placed between two plexiglass sheets, which compressed the hydrogel up to 80% of the original length. While compressing the sample, inner electrolyte solution started to come out from the pores of agarose hydrogel and hydrogel shrank. Still, in the case of placing the outer electrolyte stamp, the precipitation patterns formed as shown in the Figure 25. Although the patterns were successfully attained, in all cases we tried, during the compression the agarose sample starts to fail (tearing) and lose its structure, as can be seen in Figure 25. In the case of very low compression (< 5%), even in the absence of cracks, agarose gel deformation will not be reversible (elastic) due to poor mechanical properties of the agarose hydrogels.

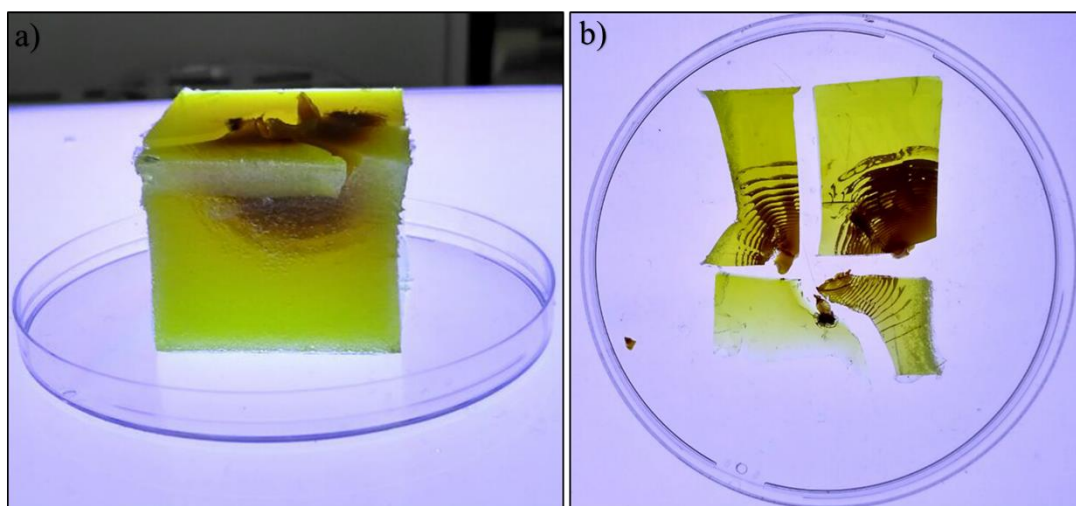


Figure 25. Cracks formed in presence of 20% mechanical deformation (compression) in cubic agarose sample (a). Thin layers of sample for rings detection (b). *Agarose = 8 w%, Inner electrolyte (potassium chromate) = 0.01 M, outer electrolyte (copper chloride) = 1 M, T = 20 °C. For details of the gel preparation and loading setup please see Chapter 2.*

### 3.1.3.2 Formation of LP and post-patterns in 3D polyacrylamide-alginate hybrid gels

Because of the failed attempt with agarose (described in the previous section), we altered the gel medium to PAA, which is more compressible. However, the conventional polyacrylamide hydrogels are not suitable for preparation of **3D** bulk hydrogels. Therefore, we augmented the gel by the addition of sodium alginate, which can boost the mechanical properties of hydrogels [45]. In this case, too, there were practical problems, i.e., in molding and demolding of prepared **3D** hydrogels the final hydrogel surface finish was always damaged. Inspired by Li Peng et al work [57] we started preparing our bulk hydrogels with a new method. In their study, Peng et al mentioned using fast reaction of  $\text{CaCl}_2$  with Sodium alginate (SA) and production of ionically cross-linked calcium alginate as a scaffold for secondary gelation, i.e. for formation of a second gel layer on the primary gel. In this method, it is possible to make a mechanically strong and reliable framework of secondarily gelated **3D** PAA-SA hybrid hydrogel. We tried making this gel by three different procedures; i) covering the surface of the molds with no filter paper, ii) with a layer of dry filter paper, and iii) with a 0.1 M  $\text{CaCl}_2$  wetted filter paper to make a shell of calcium



alginate. As illustrated in Figure 26 the best results are obtained with sample with  $\text{CaCl}_2$  wetted filter paper, providing us the best surface finish and bulk dimensions.

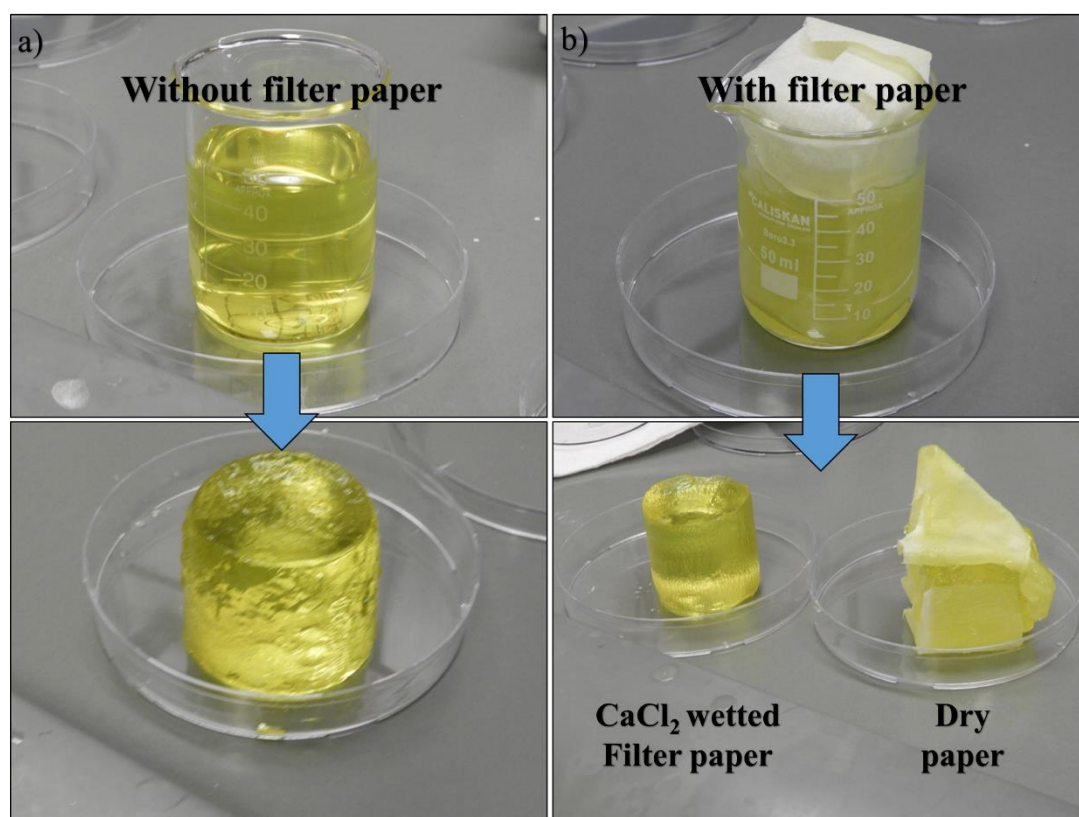


Figure 26. Effect of mold surface modification on final **3D** polyacrylamide-sodium alginate (PAA-SA) hybrid hydrogel. (a) PAA-SA, gel molded without filter paper. (b) PAA-SA hydrogels molded with filter paper. In (b) demolding is easy for both samples but in the sample with dry filter paper, separation of the gel and the filter paper is not possible. Finally, the best configuration is using  $\text{CaCl}_2$ , for which both demolding and removal of the paper are straightforward. *Inner electrolyte (potassium chromate) = 0.01 M, acrylamide = 13.5 w%, BIS = 0.056 w%, KPS = 0.187 w%, sodium alginate = 0.187 w%, TEMED = 0.0001 w%.  $T = 20\text{ }^\circ\text{C}$ . For details of the gel preparation please see Chapter 2.*

In this new **3D** PAA-SA hydrogel, LPs could be formed successfully under the same chemical conditions applied to **2D** gels as shown in Figure 27. To study the effect of mechanical deformation in **3D**, the samples were prepared in a cubic mold with 4 cm X 4 cm X 4 cm dimensions. After removing the hydrogel from mold, sample was placed in **3D** deformation setup (Figure 28), and compressed in one direction. Stamp was placed on the top surface of cube (which has not been in contact with  $\text{CaCl}_2$ )

providing the outer electrolyte (1M  $\text{CuCl}_2$ ) and sample was left for 24 hours, until which time patterns formed.

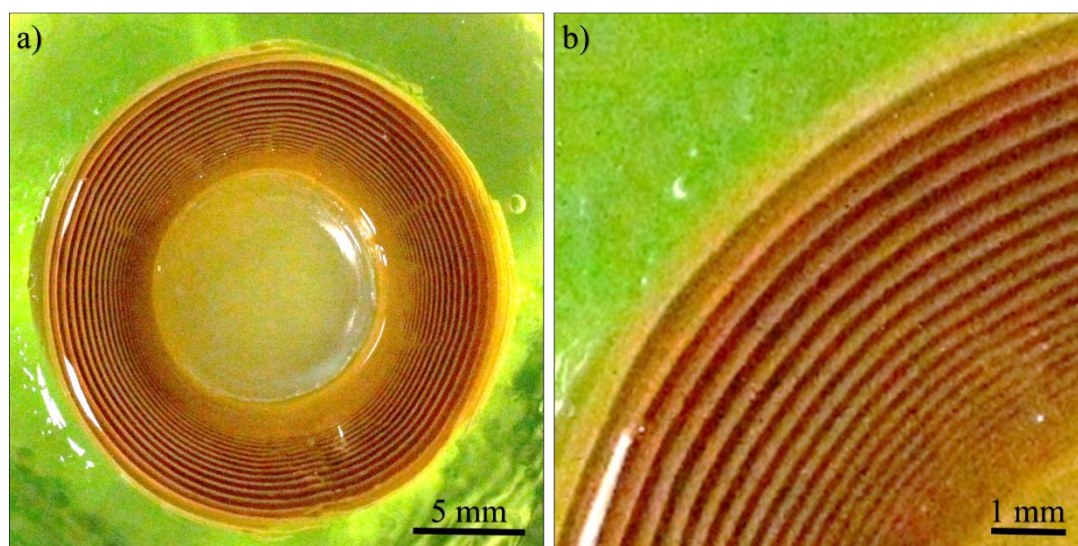


Figure 27. Formation of LP in the **3D** polyacrylamide-sodium alginate (PAA-SA) hybrid hydrogel. The cylindrical stamp is placed on the surface of the cube-shaped gel. Developing time was 24 hrs. The chemistry and the concentration of inner and outer-electrolyte are similar to **1D** and **2D** PAA hydrogels. *Inner electrolyte (potassium chromate) = 0.01 M, acrylamide = 13.5 w%, BIS = 0.056 w%, KPS = 0.187 w%, sodium alginate = 0.187 w%, TEMED = 0.0001 w%.  $T = 20\text{ }^\circ\text{C}$ . For details of the gel preparation please see Chapter 2.*

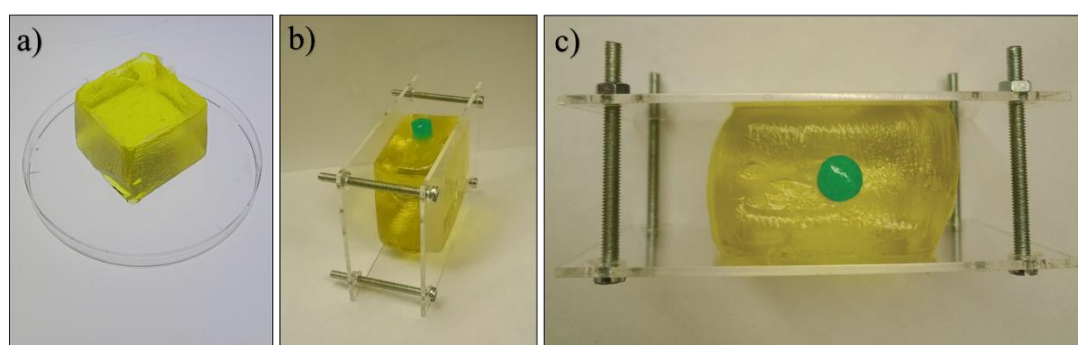


Figure 28. Mechanical deformation setup in **3D**. (a) **3D** polyacrylamide-sodium alginate (PAA-SA) hydrogel. (b) Isometric view of compression test setup. (c) Top view of compressed gel with stamp placed. *Compression = 30 %. Inner electrolyte (potassium chromate) = 0.01 M, outer electrolyte (copper chloride) = 1 M, acrylamide = 13.5 w%, BIS = 0.056 w%, KPS = 0.187 w%, sodium alginate = 0.187 w%, TEMED*

= 0.0001 w%.  $T = 20\text{ }^{\circ}\text{C}$ . For details of the gel preparation and the loading setup please see Chapter 2.

As seen in Figure 29, in the first 24 hours between placing stamp and before unloading (compression) patterns formed as concentric shells. (The hemisphere shells looked like the ones in **2D** – as concentric rings, if the patterns were observed from the top, Figure 29a)

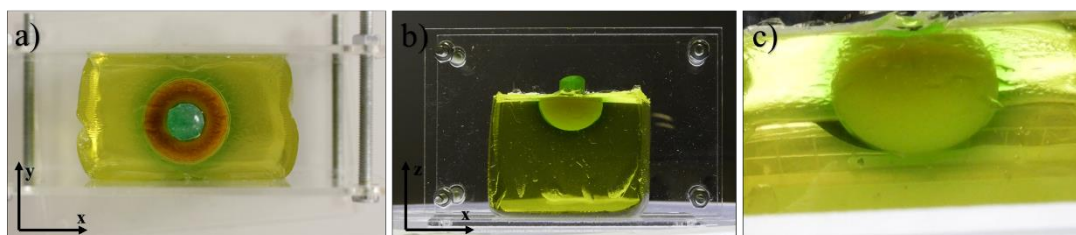


Figure 29. formation of patterns in **3D** polyacrylamide-sodium alginate (PAA-SA) gel after 24 hours with 30% compression. Concentric shell patterns form, (a) top, (b) side and (c) bottom view of the hemispherical patterns. For details of the gel preparation and loading setup please see Chapter 2.

As in the case of the **2D** patterns, upon unloading, the aspect ratio of the **3D** shells change (the patterns looks like concentric ovals). Note that, for **3D** samples the mode of mechanical action is compression rather than tension, so the aspect ratio of the rings increases to 1.0 from 1.3 (Figure 30) but an ‘expansion’ of the pattern is observed in the direction of the applied stress.

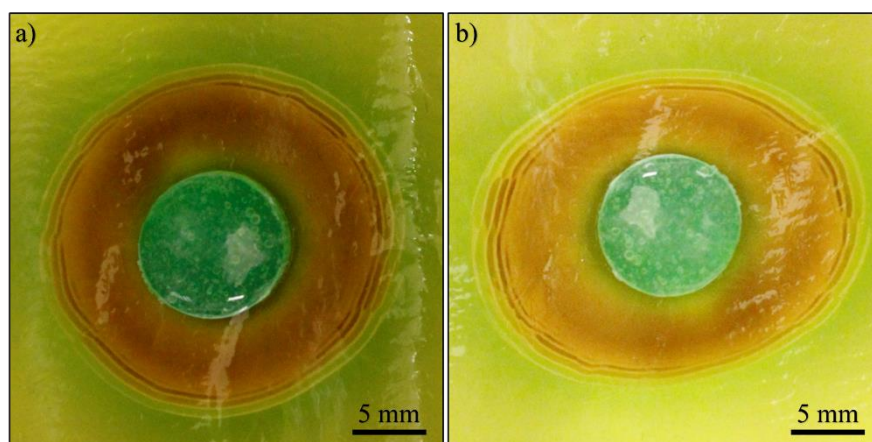


Figure 30. Photos of the LP formed upon loading and just after unloading (releasing) the compressive load. (a) Top view of pattern formed in polyacrylamide-sodium alginate (PAA-SA) **3D** hydrogel in 24 hours under a compressive load. (b) Aspect

ratio of the pattern increases (from 1.0 to 1.30) in **3D** LP pattern right after unloading. For details of the gel preparation and loading setup please see Chapter 2.

After unloading (releasing the compressive load), the **3D** sample was left for 12 more hours for the formation of the PPs, which developed by this time as concentric incomplete shells in a direction which is perpendicular to compressive load, as shown in Figure 31b, c, and d.

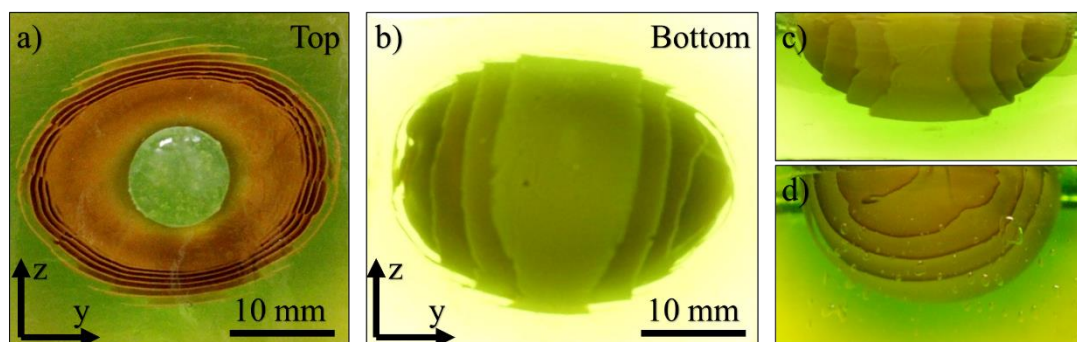


Figure 31. Formation of post-patterns in **3D** in the presence of mechanical deformation (30% compression). (a) LP patterns just after releasing the load. (b) Formation of post rings perpendicular to the stress direction, bottom view. (c) Side view of patterns perpendicular to the stress direction. (d) Side view of patterns in the stress direction. Inner electrolyte (potassium chromate) = 0.01 M, outer electrolyte (copper chloride) = 1 M, acrylamide = 13.5 w%, BIS = 0.056 w%, KPS = 0.187 w%, sodium alginate = 0.187 w%, TEMED = 0.0001 w%.  $T = 20\text{ }^{\circ}\text{C}$ . For details of the gel preparation and loading setup please see Chapter 2.

## 3.2. Elastic Deformation Tracking in 1D, 2D, and 3D hydrogels by using precipitation patterns

### 3.2.1 Determination of the tensile strain in an elastically deformed 2D hydrogel using post-patterns

As we have shown previously in section 1.4, the strain on the sample, caused by tensile loading can be determined by the change in the aspect ratio of the precipitation patterns measured after the load is released. The development of the PPs, too, can also help to detect the strain in mechanical deformation. Samples with loaded to strains of 10-50% show different configurations of the LPs and the PPs. With strains below 20%,

identification of the PPs in the whole precipitation pattern becomes hard and only in the case of very careful observation distortion in patterns width, and the change in depletion zone color and contrast can be observed, as explained in detail in section 0. However, as seen in Figure 32c in samples with strains equal to or higher than 30%, PP region, shown between the two red arrows, is more distinct with darker depletion zone and wider bands, and it consists of more number of PP bands.

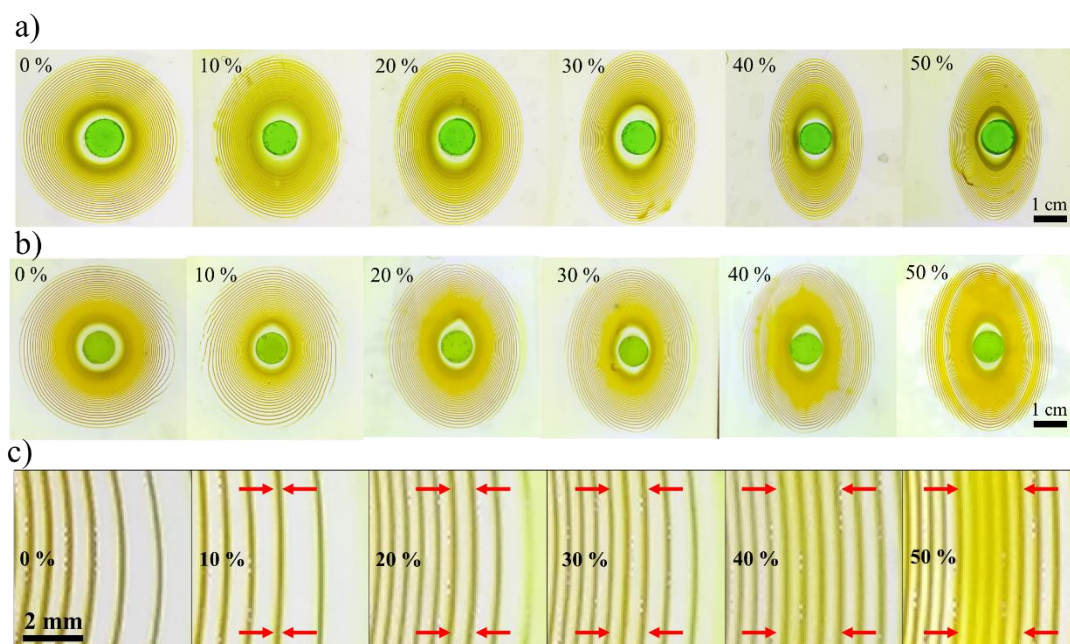


Figure 32. Post-pattern (PP) formation in the polyacrylamide (PAA) samples with applied uniaxial strain. (a) The change in the aspect ratios of the concentric LP1 formed for 24 hrs, photo taken just after unloading. (b) The formation of the PPs and LP2s (in 18 hours of waiting time) after unloading. (c) The effect of strain on the PP region's size and on the precipitation bands' width and contrast. *Inner electrolyte (potassium chromate) = 0.01 M, outer electrolyte (copper chloride) = 1 M, acrylamide = 13.5 w%, BIS = 0.056 w%, KPS = 0.187 w%, TEMED = 0.0001 w%. T = 20 °C. For details of the gel preparation and loading setup please see Chapter 2.*

### 3.2.2 Precipitation patterns in an elastically deformed 2D hydrogel under cyclic load

Using the concept of post-patterns and their different properties compared to ordinary LPs, we started to examine the possibility of using these differences for detection of time and extent of cyclic (unload/load/unload) elastic deformation in stretchable gels

in presence of cyclic deformation. For this, PAA gels were prepared the same way as gels mentioned in section 0.

We initially designed an experiment (Figure 33), which included three steps: 1) After transferring PAA gel on Ecoflex substrate, without applying any mechanical deformation, first, the stamp was placed on the hydrogel ( $T_0$ ) and the patterns were allowed to form on the unstretched hydrogel until the time  $T_1$ ; 2). A mechanical load was then applied on the gel to yield 40% strain, for a specific period of time between  $T_1$  and  $T_2$ , in which patterns continue to form in the stretched gel; 3) at  $T_2$ , the sample was unloaded and the patterns were let to develop in this unloaded state until  $T_{end}$ .

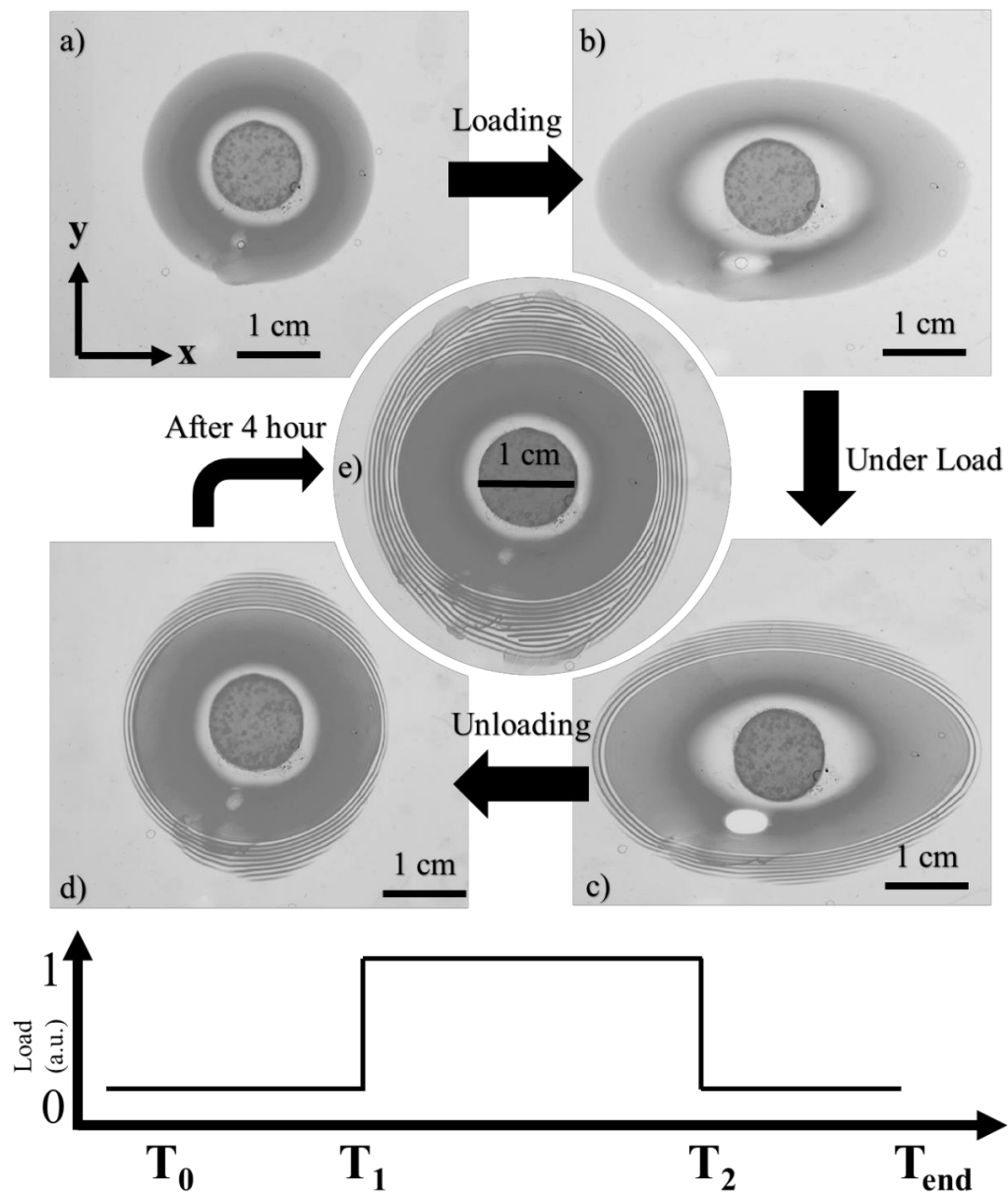


Figure 33. Pattern formation under cyclic loading. An example of a 3 step-cyclic elastic deformation of the PAA gel and the formation of the precipitation patterns.

Formation of patterns in a) 4 hrs of unloaded gel, followed by b) a stretching, which causes an overall pattern shown in (c) after 4 hrs of loading. The sample is then unloaded as shown in (d) and the patterns were left to develop for 4 hrs more in the unloaded state to yield the pattern in (e). (Here the photos are given in gray scale for a better contrast.) *Inner electrolyte (potassium chromate) = 0.01 M, outer electrolyte (copper chloride) = 1 M, acrylamide = 13.5 w%, BIS = 0.056 w%, KPS = 0.187 w%, TEMED = 0.0001 w%. T = 20 °C. For details of the gel preparation and loading setup please see Chapter 2.*

Following the same procedure for various T1 and T2 times, and with a fixed end time (T<sub>end</sub>= 12 hrs) (Table 1), different patterns were obtained as shown in Figure 34.

Table 1. The transition times used to yield different cycles of elastic deformation to obtain the precipitation patterns shown in Figure 20. T<sub>end</sub>=12 hours (fixed).

Set No.	1	2	3	4	5
T1	4	4	6	6	8
T2	6	8	8	10	10

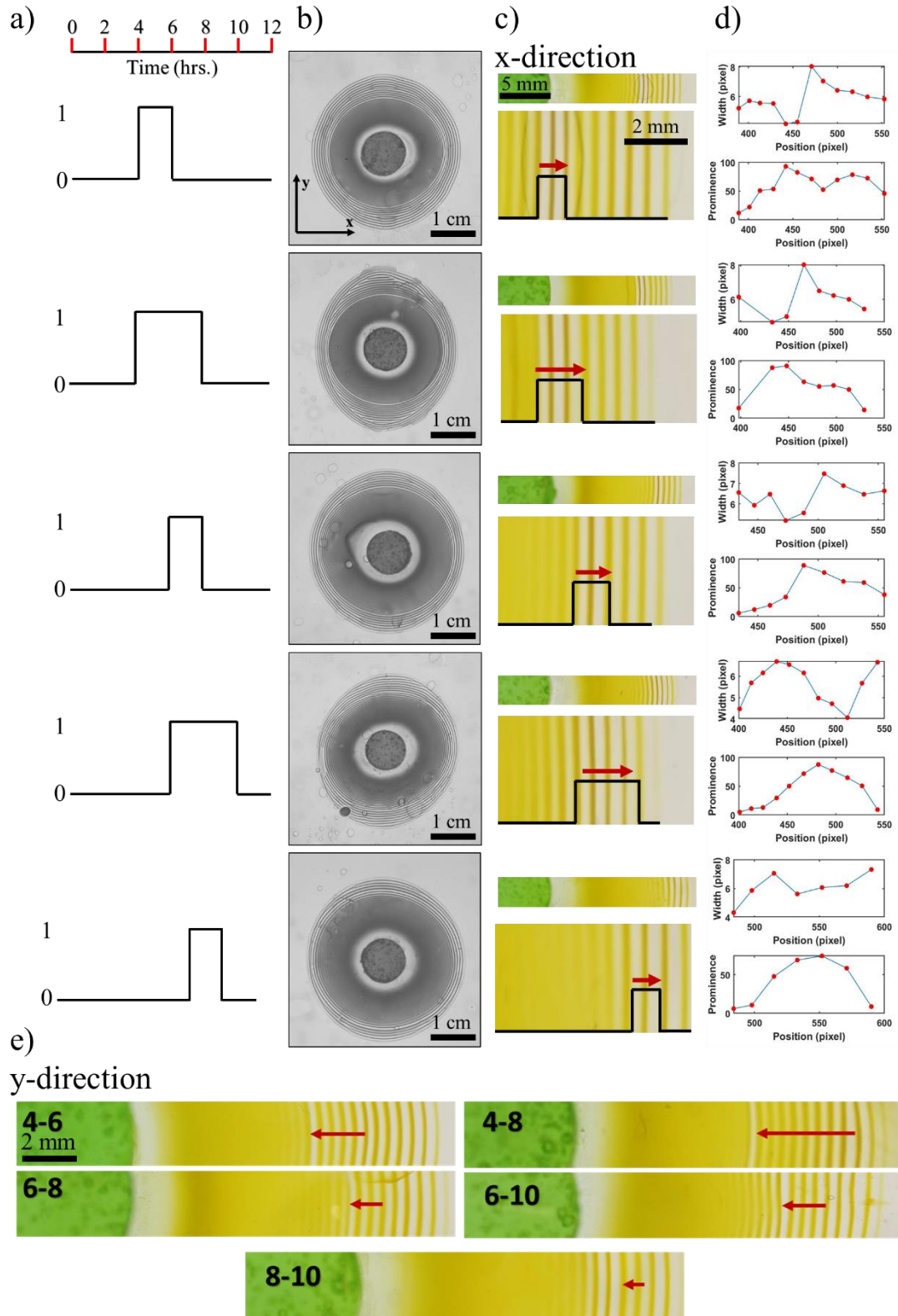


Figure 34. Cyclic deformation in **2D** polyacrylamide (PAA) hydrogels. Samples are mechanically loaded/unloaded (stretched/released) in x-direction through cycles as shown in (a); Vertical axis 0 = unloaded (released/unstretched), and 1 = loaded (stretched) sample. (b) Overall patterns formed during the corresponding loading



cycles. (c) A magnification of the patterns formed in cyclic loading and unloading (x-direction). (d) Peak analysis of the PP formed, including peak width and prominence analysis of PP (e) PP formation in y-direction (perpendicular to uniaxial loading) (The photos are given in gray-scale for better contrast). *Inner electrolyte (potassium chromate) = 0.01 M, outer electrolyte (copper chloride) = 1 M, acrylamide = 13.5 w%, BIS = 0.056 w%, KPS = 0.187 w%, TEMED = 0.0001 w%. T = 20 °C. For details of the gel preparation and the loading setup please see Chapter 2.*

The close-up images of the LPs obtained through different deformation cycles (Figure 34) and ‘the trends’ that can be obtained through these images show that; 1) The ***time of applied load*** can be determined by tracking the starting point of the PPs; the PP in the overall pattern appears as the latter bands when T1 (starting time of deformation) is longer (shown by the beginning point of the red arrows in the figure); 2) ***the duration of the loading*** can be determined by the number of the PP bands; more bands happen when T1-T2 duration is higher (denoted by the length of the red arrow in the figure); and 3) ***the direction of the applied stress*** can be also determined by close inspection of the bands (displayed by the direction of the red arrows in the Figure 34c and e). The latter is a result of the positive Poisson ratio of the gel. That is; in the **2D** setup, when the uniaxial load is exerted on the gel in the x-direction, the gels is elongated in this direction, at the same time, the gel is compressed in the direction perpendicular to the direction of applied stress (y-direction).

### **3.2.3 Precipitation patterns in an elastically deformed 1D hydrogel under cyclic load**

As mentioned earlier in section 0, post-pattern region can form in both stretching and compression in **2D**, and **3D**. However, the best visualization of the mechanical effect can still be made in **1D**, since the patterns appear as very regular, parallel bands in **1D**. Therefore, we tried to show the elastic deformation tracking (cyclic load) also by the **1D** setup. 5 samples were taken to show the effect of the applied different cyclic loads. Stamp was placed on a hydrogel, which was then loaded (stretched) and unloaded (released) at specific T1 and T2 times, respectively, with two- or four-hour intervals as shown in Figure 35a. As can be seen in Figure 35b, the different cycles can lead to different precipitation patterns. In the regions that post-patterns were formed due to the mechanical loading of the hydrogel between T1 and T2, LPs formed were found

to be thinner and in higher contrast to the depletion zone at the background. After unloading the samples and waiting for the given time period, a new type of precipitation pattern, PPs, formed which could easily be distinguished due to the increase in the band width and decreasing contrast of the intra-pattern regions (depletion zone).

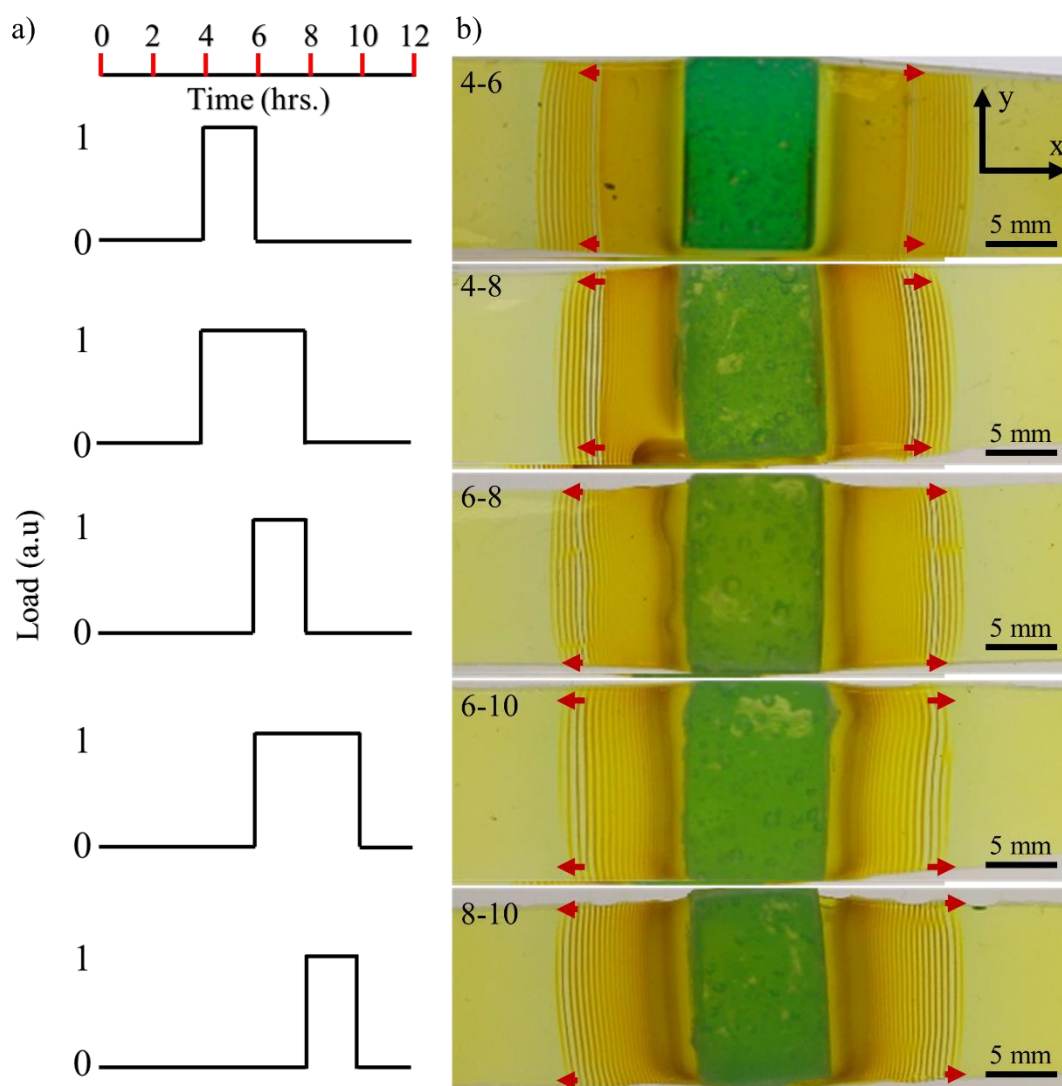


Figure 35. Cyclic deformation in **1D** polyacrylamide (PAA) hydrogels. Samples are mechanically loaded/unloaded (stretched/released) in x-direction through cycles as shown in (a); Vertical axis 0 = unloaded (released/unstretched), and 1 = loaded (stretched) sample. (b) The patterns formed in cyclic loading and unloading (x-direction). *Inner electrolyte (potassium chromate) = 0.01 M, outer electrolyte (copper chloride) = 1 M, acrylamide = 13.5 w%, BIS = 0.056 w%, KPS = 0.187 w%, TEMED*

= 0.0001 w%.  $T = 20\text{ }^{\circ}\text{C}$ . For details of the gel preparation and loading setup please see Chapter 2.

In Figure 36, more detailed demonstration of the post-patterns structure can be seen. Data analysis of these patterns showed, how one can use the intensity of the peaks and the pattern width to locate the position of post-pattern (due to loading and stretching) in such a sample.

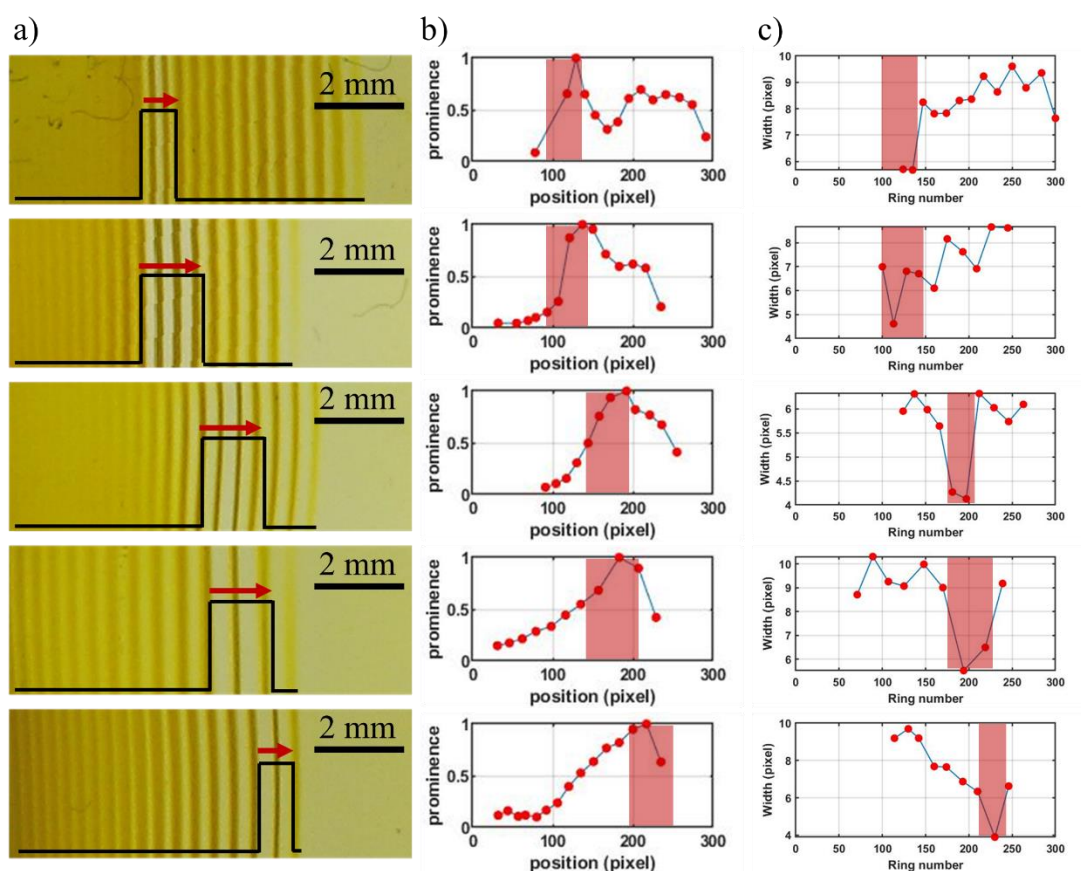


Figure 36. A detailed demonstration of the PP formation in cyclic loading and unloading. (a) Magnified view of the patterns shown in Figure 35. (b) Peak prominence and (c) peak width analysis of the patterns. *Inner electrolyte (potassium chromate) = 0.01 M, outer electrolyte (copper chloride) = 1 M, acrylamide = 13.5 w%, BIS = 0.056 w%, KPS = 0.187 w%, TEMED = 0.0001 w%.  $T = 20\text{ }^{\circ}\text{C}$ . For details of the gel preparation and loading setup please see Chapter 2.*

### **3.3. Removing patterns**

So far, our ability for tracking mechanical deformations and dimensional transformations were limited to the formation of patterns right after placing the stamps. Formed patterns stayed at the locations they form on the gel, until the hydrogel exists. However, this permanent patterns can hinder transparency of samples in some applications. Removing and reproducing these patterns may help for more accurate tracking and time saving. In addition, it can eliminate potential further chemical reactions that can take place between the remaining of inner and outer electrolytes, and the precipitate, and the chemicals in the environment, e.g., when (if) the gels are used as mechanical deformation sensors on other substrates. In this respect, dissolving patterns can help us to remove these chemicals left in the gel. In the literature, it is mentioned that EDTA can be useful in removing copper hydroxide patterns formed in sodium polyacrylate hydrogel [58]. Here considering the chemical nature of the PAA hydrogels, we chose three different solutions ( $\text{NH}_3$ ,  $\text{CH}_3\text{COOH}$ ,  $\text{HCl}$ ), which can dissolve and wash the formed pattern.

### **3.4. Pyrrole polymerization on the previously formed precipitation patterns**

So far, we discussed the possibility of using post-pattern formation for tracking the time, extent and type of a mechanical deformation. PPs with their unique properties like their equidistant spacing, make it possible to develop and track controlled patterns. Patterning is a very important subject of research with its diverse applications in science and industry. However, many of these techniques such as, lithography [59], laser engraving [60], printing and so forth, are very expensive. LPs and PPs together have the potential to replace many of such patterning techniques by providing the possibility of spontaneous formation of a controlled pattern. Herein, as an example for potential application of Liesegang periodic patterns, we examined the polymerization of pyrrole on PAA hydrogels patterned with  $\text{CuCrO}_4$  LPs. Polypyrrole has been center of attention in scientific community for its electrical properties, and as a conducting polymer has been explored for many applications like spintronics, memory devices, sensors, microwave absorption devices, and electromagnetic shielding [61,62]. We showed one example of such a straightforward patterning of polypyrrole, with precipitation patterns formed with and without mechanical deformation. The essence

of the polypyrrole formation and deposition on the patterns lies in the fact that  $\text{Cu}^{2+}$  in  $\text{CuCrO}_4$  precipitation in LPs and PPs can act as a polymerization catalyst, which results in pyrrole polymerization on them. Just by just dipping the patterned hydrogel in the pyrrole solution the polypyrrole formation and patterning can be achieved (Figure 37). Addition of minute amounts of HCl can accelerate polymerization by decomposition of  $\text{CuCrO}_4$  to  $\text{Cu}^{2+}$ , providing more  $\text{Cu}^{2+}$  for the reaction. Finally, we may safely conclude that the successful patterning of the polypyrrole with different spacings can be achieved by this approach.

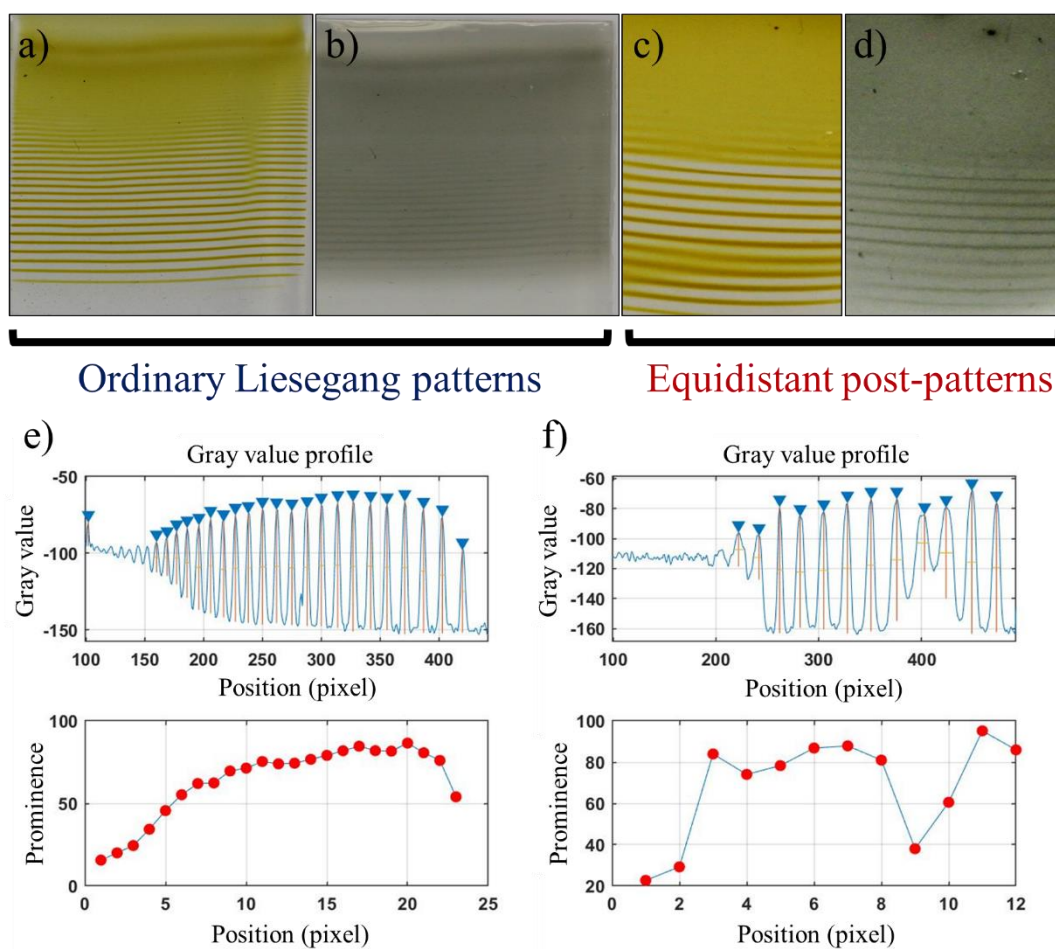


Figure 37. Polymerization of pyrrole on polyacrylamide (PAA) hydrogel with LPs formed. (a-b) Polypyrrole formation on regular LPs. (c-d) Polypyrrole formation on the patterns developed on mechanically deformed hydrogel. Peak analysis of LP formed on PAA (e) without mechanical deformation, and (f) with mechanical deformation. In all cases, the samples with patterns were dipped in pyrrole solution (pyrrole = 0.1 M, HCl = 0.1 mM). Inner electrolyte (potassium chromate) = 0.01 M, outer electrolyte (copper chloride) = 1 M, acrylamide = 13.5 w%, BIS = 0.056 w%,

*KPS = 0.187 w%, TEMED = 0.0001 w%. T = 20 °C. For details of the gel preparation please see Chapter 2.*

## CHAPTER 4

### 4. CONCLUSION

In this study, it was shown that mechanical deformation on stretched polyacrylamide gels can be used to control the simultaneous formation of the Liesegang patterns in the gel medium. Then the changes noted were used for detection and tracking elastic mechanical deformation in the hydrogels. Finally, the patterns in the gels were used to direct the polymerization of pyrrole on the gel surfaces; the control of patterns via mechanical deformation provided a way to design polypyrrole bands with two different spacings.

Together with the aspect ratio changes upon unloading, the discovery of post-patterns that form as pattern irregularities after unloading (and their unique properties like patterns width, and patterns spacing) provided an information-rich platform to track both tensile and compressive elastic mechanical deformation in **1D**, **2D** and **3D** system. This system enabled to extract spatial, temporal, and duration in an unprecedented way. This work also provided an example of interesting phenomenon of pattern formation, to be explored, such as the PPs that appear surprisingly as incomplete shells upon compressive deformation of **3D** gels.

In general, the discovery of post-patterns will allow researchers to control precipitation patterns, i.e., their bandwidth and bands spacings. As we have shown with the polypyrrole patterning, this new method can be a ‘chemical patterning’ in addition to many patterning techniques such as lithography or laser engraving. The combination of pyrrole polymerization on precipitation patterns with control over chemistry of precipitation patterns and controlled anisotropies resulting from mechanical deformation can be a good starting point for more research on pattern

forming systems, leading to patterns not directly available through precipitation reactions.

Overall, we displayed a system, which contributed to the fundamental knowledge on the precipitation phenomena and provided examples of practical ramifications of these phenomena that, we hope, can further be elaborated in the future.



## 5. REFERENCES

- [1] Whitesides GM, Grzybowski B. Self-assembly at all scales. *Science* 2002;295:2418–21. doi:10.1126/science.1070821.
- [2] Shinbrot T, Muzzio FJ. Noise to order. *Nature* 2001;410:251–8. doi:10.1038/35065689.
- [3] Walliser RM, Boudoire F, Orosz E, Tóth R, Braun A, Constable EC, et al. Growth of nanoparticles and microparticles by controlled reaction-diffusion processes. *Langmuir* 2015;31:1828–34. doi:10.1021/la504123k.
- [4] Sadek S, Sultan R. Liesegang patterns in nature: A diverse scenery across the sciences. vol. 661. 2010.
- [5] Rácz Z. Formation of Liesegang patterns. *Phys A Stat Mech Its Appl* 1999;274:50–9. doi:10.1016/S0378-4371(99)00432-X.
- [6] Morse HW, Pierce GW. Diffusion and Supersaturation in Gelatine. *Phys Rev (Series I)* 1903;17:129–50. doi:10.1103/PhysRevSeriesI.17.129.
- [7] Jablczynski CK. No Title. *Bull Soc Chim Fr* 1923;33:1592.
- [8] Mueller SC, Kai S, Ross J. Periodic precipitation patterns in the presence of concentration gradients. 1. Dependence on ion product and concentration difference. *J Phys Chem* 1982;86:4078–87. doi:10.1021/j100217a038.
- [9] Sultan RF, Abdel-Rahman AFM. On dynamic self-organization: Examples from magmatic and other geochemical systems. *Lat Am J Solids Struct* 2013;10:59–73. doi:10.1590/S1679-78252013000100006.
- [10] Saad M, Sa A, Sultan R. Revisited Chaos in a Diffusion – Precipitation – Redissolution Liesegang System 2020:5–9. doi:10.1021/acs.jpca.8b03229.
- [11] Bensemam IT, Fialkowski M, Grzybowski BA. Wet stamping of microscale periodic precipitation patterns. *J Phys Chem B* 2005;109:2774–8. doi:10.1021/jp047885b.
- [12] Feeney R, Schmidt SL, Strickholm P, Chadam J, Ortoleva P. Periodic

- precipitation and coarsening waves: Applications of the competitive particle growth model. *J Chem Phys* 1983;78:1293–311. doi:10.1063/1.444867.
- [13] Sadek S, Sultan R. Liesegang patterns in nature: A diverse scenery across the sciences. *Precip Patterns React Syst* 2010;661:1–43.
- [14] Ramírez-Álvarez E, Montoya F, Buhse T, Rios-Herrera W, Torres-Guzmán J, Rivera M, et al. On the dynamics of Liesegang-type pattern formation in a gaseous system. *Sci Rep* 2016;6:1–13. doi:10.1038/srep23402.
- [15] Grzybowski BA, Wiley InterScience (Online service). *Chemistry in Motion*. vol. 91. Wiley; 2016. doi:10.1021/cen-09134-ad11.
- [16] Wochenschr RL-N, 1896 undefined. Uber einige eigenschaften von gallerten. *CiNiiAcJp* n.d.
- [17] Yan H, Zhao Y, Qiu C, Wu H. Micropatterning of inorganic precipitations in hydrogels with soft lithography. *Sensors Actuators B Chem* 2008;132:20–5. doi:10.1016/J.SNB.2008.01.002.
- [18] Morse HW. Periodic Precipitation in Ordinary Aqueous Solutions. *J Phys Chem* 1929;34:1554–77. doi:10.1021/j150313a016.
- [19] Isemura T. Studies on Rhythmic Precipitates. *Bull Chem Soc Jpn* 1939;14:179–237. doi:10.1246/bcsj.14.179.
- [20] Zhang H, Zhan K, Chen Y, Chen G, Zhou X, Liu J, et al. Three dimension Liesegang rings of calcium hydrophosphate in gelatin. *J Sol-Gel Sci Technol* 2014;71:597–605. doi:10.1007/s10971-014-3411-8.
- [21] Goodeve CF, Eastman AS, Dooley A. The reaction between sulphur trioxide and water vapours and a new periodic phenomenon. *Trans Faraday Soc* 1934;30:1127. doi:10.1039/tf9343001127.
- [22] Spatz EL, Hirschfelder JO. Liesegang Ring Formation Arising from Diffusion of Ammonia and Hydrogen Chlorine Gases through Air. *J Chem Phys* 1951;19:1215–1215. doi:10.1063/1.1748519.
- [23] Stern KH. Liesegang phenomenon [4]. *Science* (80- ) 1959;130:726. doi:10.1126/science.130.3377.726.
- [24] Turing AM. The chemical basis of morphogenesis. *Bull Math Biol* 1990;52:153–97. doi:10.1007/BF02459572.
- [25] Shimizu Y, Matsui J, Unoura K, Nabika H. Liesegang Mechanism with a Gradual Phase Transition 2017:1–4. doi:10.1021/acs.jpcc.7b01275.
- [26] Ferenc I, Lagzi I. Models of Liesegang pattern formation 2010:10.

- [27] Thomas S, Varghese G, Lagzi I. The width of Liesegang bands: A study using moving boundary model and simulation. *Pramana - J Phys* 2012;78:135–45. doi:10.1007/s12043-011-0204-2.
- [28] Antal T, Droz M, Magnin J, Pekalski A, Rácz Z. Formation of Liesegang patterns: simulations using a kinetic Ising model. *J Chem Phys* 2001;114:3770–5. doi:10.1063/1.1342858.
- [29] Nakouzi E, Steinbock O. Self-organization in precipitation reactions far from the equilibrium n.d. doi:10.1126/sciadv.1601144.
- [30] Smoukov SK, Lagzi I, Grzybowski BA. Independence of primary and secondary structures in periodic precipitation patterns. *J Phys Chem Lett* 2011;2:345–9. doi:10.1021/jz101679t.
- [31] Duley JM, Fowler AC, Moyles IR, O'Brien SBG. On the Keller–Rubinow model for Liesegang ring formation. *Proc R Soc A Math Phys Eng Sci* 2017;473:20170128. doi:10.1098/rspa.2017.0128.
- [32] Lagzi I. Controlling and Engineering Precipitation Patterns. *Langmuir* 2012;28:3350–4. doi:10.1021/la2049025.
- [33] Büki A, Kárpáti-Smidróczki É, Zrínyi M. Computer simulation of regular Liesegang structures. *J Chem Phys* 1995;103:10387–92. doi:10.1063/1.469875.
- [34] Matalon R, Packter A. The Liesegang phenomenon. I. Sol protection and diffusion. *J Colloid Sci* 1955;10:46–62. doi:10.1016/0095-8522(55)90076-3.
- [35] Badr L, Sultan R. Ring morphology and pH effects in 2D and 1D Co(OH)<sub>2</sub> liesegang systems. *J Phys Chem A* 2009;113:6581–6. doi:10.1021/jp8094984.
- [36] Shreif Z, Mandalian L, Abi-Haydar A, Sultan R. Taming ring morphology in 2D Co(OH)<sub>2</sub> Liesegang patterns. *Phys Chem Chem Phys* 2004;6:3461–6. doi:10.1039/b404064c.
- [37] Toramaru A, Harada T, Okamura T. Experimental pattern transitions in a Liesegang system. *Phys D Nonlinear Phenom* 2003;183:133–40. doi:10.1016/S0167-2789(03)00139-8.
- [38] Kárpáti-Smidróczki E, Büki A, Zrínyi M. Pattern forming precipitation in gels due to coupling of chemical reactions with diffusion. *Colloid Polym Sci* 1995;273:857–65. doi:10.1007/BF00657635.
- [39] Smoukov SK, Bitner A, Campbell CJ, Kandere-Grzybowska K, Grzybowski BA. Nano- and microscopic surface wrinkles of linearly increasing heights prepared by periodic precipitation. *J Am Chem Soc* 2005;127:17803–7.

doi:10.1021/ja054882j.

- [40] Makki R, Al-Ghoul M, Sultan R. Propagating fronts in thin tubes: Concentration, electric, and pH effects in a two-dimensional precipitation pulse system. *J Phys Chem A* 2009;113:6049–57. doi:10.1021/jp8087226.
- [41] Lagzi I. Formation of Liesegang patterns in an electric field. *Phys. Chem. Chem. Phys.*, vol. 4, The Royal Society of Chemistry; 2002, p. 1268–70. doi:10.1039/b109835g.
- [42] Al-Ghoul M, Sultan R. Front propagation in patterned precipitation. 2. Electric effects in precipitation-dissolution patterning schemes. *J Phys Chem A* 2003;107:1095–101. doi:10.1021/jp022433p.
- [43] Bena I, Droz M, Rácz Z. Formation of Liesegang patterns in the presence of an electric field. *J Chem Phys* 2005;122:204502. doi:10.1063/1.1899644.
- [44] Kanazawa Y, Asakuma Y. Diffusion and Reactions in Liesegang Systems Under Microwave Irradiation. *J Cryst Process Technol* 2014;2:4–7. doi:10.4236/jcpt.2014.42009.
- [45] Sun J-Y, Zhao X, Illeperuma WRK, Chaudhuri O, Oh KH, Mooney DJ, et al. Highly stretchable and tough hydrogels. *Nature* 2012;489:133–6. doi:10.1038/nature11409.
- [46] Calvert P. Hydrogels for soft machines. *Adv Mater* 2009;21:743–56. doi:10.1002/adma.200800534.
- [47] Raymond S, Weintraub L. Acrylamide gel as a supporting medium for zone electrophoresis. *Science* (80- ) 1959;130:711. doi:10.1126/science.130.3377.711.
- [48] Vanchugova L V., Valuev LI, Valuev IL, Talyzenkov YA. Control of the structure of polyacrylamide hydrogel. *Polym Sci Ser B* 2013;55:77–80. doi:10.1134/S156009041302005X.
- [49] Valade D, Wong LK, Jeon Y, Jia Z, Monteiro MJ. Polyacrylamide hydrogel membranes with controlled pore sizes. *J Polym Sci Part A Polym Chem* 2013;51:129–38. doi:10.1002/pola.26311.
- [50] Lira LM, Martins KA, Torresi SIC de. Structural parameters of polyacrylamide hydrogels obtained by the Equilibrium Swelling Theory. *Eur Polym J* 2009;45:1232–8. doi:10.1016/J.EURPOLYMJ.2008.12.022.
- [51] Li Y, Li X, Zheng L, Wang L, Zhang X, Xu F. Polyacrylamide/GelMA Hydrogel Templates for Breast Cancer Cell Spheroids Fabrication. *J*

- Nanotechnol Eng Med 2016;6:034501. doi:10.1115/1.4031898.
- [52] Ko YGUN, Choi UNGSU, Park YS, Woo JEWAN. Fourier Transform Infrared Spectroscopy Study of the Effect of pH on Anion and Cation Adsorption onto Poly ( acrylo- amidino diethylenediamine ) 2010:2010–8.
- [53] Ashirov R. Chemical and mechanical control of liesegang patterns in polyacrylamide hydrogels 2018.
- [54] Chao TH, March J. A study of polypyrrole synthesized with oxidative transition metal ions. *J Polym Sci Part A Polym Chem* 1988;26:743–53. doi:10.1002/pola.1988.080260306.
- [55] Schneider CA, Rasband WS, Eliceiri KW. NIH Image to ImageJ: 25 years of image analysis. *Nat Methods* 2012;9:671–5. doi:10.1038/nmeth.2089.
- [56] Droz M, Magnin J, Zrinyi M. Liesegang patterns: Studies on the width law. *J Chem Phys* 1999;110:9618. doi:10.1063/1.478927.
- [57] Peng L, Liu Y, Huang J, Li J, Gong J, Ma J. Microfluidic fabrication of highly stretchable and fast electro-responsive graphene oxide/polyacrylamide/alginate hydrogel fibers. *Eur Polym J* 2018;103:335–41. doi:10.1016/J.EURPOLYMJ.2018.04.019.
- [58] Palleau E, Morales D, Dickey MD, Velev OD. Reversible patterning and actuation of hydrogels by electrically assisted ionoprinting. *Nat Commun* 2013;4:1–7. doi:10.1038/ncomms3257.
- [59] Wu ZL, Moshe M, Greener J, Therien-Aubin H, Nie Z, Sharon E, et al. Three-dimensional shape transformations of hydrogel sheets induced by small-scale modulation of internal stresses. *Nat Commun* 2013;4:1586–7. doi:10.1038/ncomms2549.
- [60] Hanlon RT, Shepherd RF, Pikul JH, Cohen I, Bai H, Li S. Stretchable surfaces with programmable 3D texture morphing for synthetic camouflaging skins. *Science (80- )* 2017;358:210–4. doi:10.1126/science.aan5627.
- [61] Kasisomayajula S, Jadhav N, Gelling VJ. In situ preparation and characterization of a conductive and magnetic nanocomposite of polypyrrole and copper hydroxychloride. *RSC Adv* 2016;6:967–77. doi:10.1039/c5ra20441k.
- [62] Jain R, Jadon N, Pawaiya A. Polypyrrole based next generation electrochemical sensors and biosensors: A review. *TrAC - Trends Anal Chem* 2017;97:363–73. doi:10.1016/j.trac.2017.10.009.